Joint Network Capacity Region for Cognitive Networks Heterogeneous Environments and RF-environment Awareness

Yuchul Kim, *Student Member* and Gustavo de Veciana *Fellow*, IEEE
The University of Texas at Austin
Email: {yuchul.kim@mail,gustavo@ece}.utexas.edu

***Abstract*—In this paper, we characterize the joint network capacity region for a licensed broadcast (primary) and ad hoc cognitive (secondary) network in a heterogeneous environment, including indoor and outdoor transmissions, under various spectrum (white space) detection techniques. Each technique delivers a different degree of RF-environment awareness - the more a device knows about its environment the larger the network capacity region. To quantify the gains, we develop a simple stochastic model capturing the interdependency amongst primary and secondary nodes and compare their joint capacity. Cognitive devices using the classical signal energy detection method are shown to perform poorly due to limitations on detecting primary transmitters in environments with indoor shadowing. This can be circumvented through direct use (e.g., database access) of location information on primary transmitters, or better yet, on that of primary receivers. The specific capacity trade-off between primary and secondary networks depends on white space detection techniques, resulting in joint network capacity regions which range from complement convex to linear to (almost) convex. Our results show that, for example, the gain of positioning-assisted method over signal energy detection is 76% and the gain of receiver location-aware approach is 177% when the density of primary transmitters is $2 \times 10^{-10} m^{-2}$, the indoor shadowing level is $-10dB$, and the fraction of indoor nodes is 0.5. Furthermore we show that if cognitive devices have positioning information then the secondary network's capacity increases monotonically with increased indoor shadowing in the environment. By contrast for devices relying solely on signal energy detection the secondary network's capacity can be non-monotonic in the indoor shadowing attenuation. These are the first analytical results quantifying, albeit for simple heterogeneous environmental model, the capacity gains one can expect when cognitive devices leverage additional information.**

***Index Terms*—Cognitive network model, stochastic geometry, transmission capacity, network capacity region, RF environment awareness**

I. Introduction

An irony of the current wireless era is that allocated spectrum is substantially underutilized while very little spectrum is available for new wireless applications. For this reason, cognitive radio techniques which take advantage of underutilized spectrum have received lots of attention [1]–[4]. A cognitive radio in this paper will refer to a wireless transceiver designed to operate opportunistically in a frequency band which has been allocated to licensed devices. To allow such opportunistic operation, strong requirements are placed on cognitive devices so as to protect licensed receivers from interference. Detecting underutilized spectrum or white space, while protecting licensed receivers, is a challenging task. The fundamental difficulty in detecting white space is *uncertainty* in the environment e.g., noise, shadowing, fading, licensed receivers' locations, limited detection capability of wireless devices, etc. Perhaps the simplest solution to this problem, explained in more detail later, is to apply a threshold to the measured licensed transmitter's signal energy. To avoid interference to primary receivers, one can make the cognitive radios very sensitive by reducing their signal energy detection threshold. However, this results in a large exclusion region around each primary transmitter, inside which no cognitive devices are allowed to transmit [5]. The performance of this simple method is particularly poor when the secondary devices must contend with uncertainty and heterogeneity, e.g., inside/outside, environments. Circumventing this problem requires a fundamentally different approach. Indeed the uncertainty can be significantly reduced if cognitive devices have more detailed information on their operating environment. We shall refer to such cognitive devices as RF-environment aware.

In this paper, we will study the interplay between the transmission capacities of primary and secondary nodes, under different levels of RF-environment awareness. Our aim is to quantify the capacity and understand the impact of various system parameters. In particular three white space detection methods for secondary nodes are considered and gains are evaluated in terms of the joint network capacity region.

Related Work. In this paper we explore the capacity of cognitive wireless networks from spatial perspective. A spatial model is considered reflecting various physical characteristics of wireless networks such as signal attenuation, interference, heterogeneous environment (indoor/outdoor), geographical locations of nodes. This types of models have been used in evaluating the capacity of *networks*.

In [6], and numerous subsequent papers, see survey in [7], various spatial models have been introduced, where nodes are randomly distributed on the plane and signal propagating in space is attenuated based on an attenuation factor and the propagation distance. However most of this work focuses on capacity scaling for homogeneous networks. Recent work by [8], [9], also focuses on scaling laws but for "two networks with different access priority" in a cognitive network context. In their work, primary and secondary networks are found to have the same capacity scaling law $\Theta(\sqrt{n/\log n})$ and $\Theta(\sqrt{m/\log m})$ where n and m correspond to the pri-

Manuscript received Dec. 1, 2009; revised May 24, 2010. This work of Yuchul Kim is supported by a grant of the AFOSR Award FA9550-07-1-0428 and NSF Award NSF CNS-0509355. The authors are with the Wireless Networking and Communication Group, Dept. of Electrical and Computer Engineering of The University of Texas at Austin, Austin, TX, 78712-1157 USA (e-mail:yuchul.kim@mail.utexas.edu, gustavo@ece.utexas.edu).

mary/secondary receiver densities. While these works capture the scaling behavior of network capacity, they abstract detailed interactions and capacity tradeoffs between the two networks, which in turn are usually quite sensitive to system parameters. By contrast, [10], [11] study trade-offs in the transmission capacity, see e.g., [12], for models of coexisting networks capturing some degree of interaction - their work suggests capacity tradeoffs are roughly linear. However, in their work, secondary nodes do not benefit from a cognition function, so the resulting linear tradeoff seems natural. Without some type of white space detection function (or overlay approach) spectrum sharing will be inefficient. Clearly the key practical question here is understanding and optimizing the capacity of the system under various white space detection techniques.

There have been numerous efforts towards optimizing parameter selection in such networks, e.g., transmission power [13], [14] or primary exclusion zone (equivalently, the signal energy detection threshold[1]). The analysis and insights of [5], [16], are limited due to remaining uncertainties, e.g., noise, interference, shadowing [17]. To reduce uncertainty, [18]–[21] have suggested the use of additional information, which is either obtained on fly or preloaded on cognitive devices. In these work, cognitive devices can access or have some form of database with information on the environment, for instance but not limited to, the geographical information and availability of spectrum usage opportunities (or the strength of primary signal) at various locations, the characteristics of primary devices, usage pattern of licensed bands, statistics of channel availability, and spectrum sharing policy. The most effective approach, among these, may be letting the cognitive devices know the exact locations of primary receivers to be protected. As long as they are safe from interference, cognitive devices can operate freely. The work of [22] shows an approach to detect passive receivers like televisions by detecting the leakage power of the passive receivers' oscillators. They suggested the use of sensors detecting the leakage power and sending weak beacon like signals indicating their existence to nearby cognitive devices.

Other techniques have been proposed to help cognitive devices reduce the chances of mis-detection and false alarm causing poor utilization of white space. Still, the key question is how to *quantify* the relative benefits of these techniques. The work in [23] attempts to compare the data base access approach in [19] versus the pure signal energy detection approach in [5] but their model is limited to a *single* primary transmitter and receiver pair. In a similar setting, [24] explores the impact of imperfect additional information on the performance of cognitive radio systems. They showed via simulations the tradeoff between the resolution of radio environment information and performance of cognitive radios. We summarize the key contributions of this paper as follows.

Contributions. First, we provide a simple stochastic model that captures the inter-dependency between two networks with multiple primary and secondary nodes with different

[1]In [15], FCC requires the detection threshold low enough to detect even weak TV signal as low as -114dBm. In this paper, we study the performance of cognitive networks under various detection thresholds (or detection radii). This permits us to evaluate how this parameter impacts network capacity.

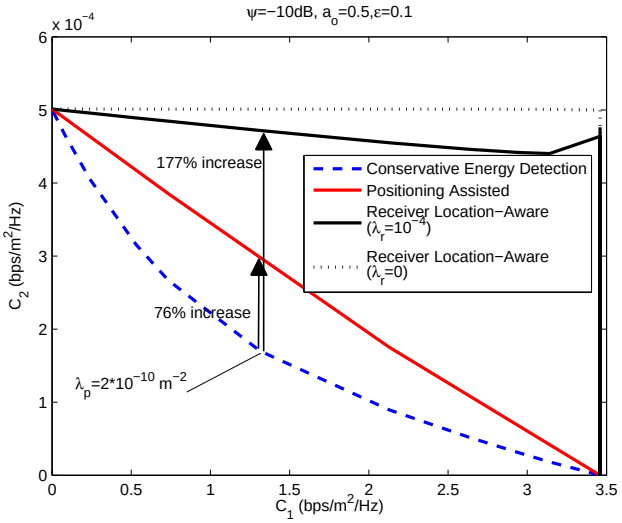

Fig. 1: The joint network capacity region of primary (C_1) and secondary capacity (C_2) was shown under -10dB of indoor shadowing for three different white space detection techniques. 50% of STxs are indoor and remaining 50% are outdoor. λ_r denotes the density of primary receivers. When the density of primary transmitter is $\lambda_p = 2 \times 10^{-10}$, the gain of positioning-assisted technique to signal energy detection technique is 76%, and that of receiver location-aware technique is 177%.

access priorities. The model is rich enough to capture the impact of heterogeneous indoor or outdoor environment on secondary nodes' white space detection techniques. The outage probabilities and joint network capacity region for primary and secondary nodes are derived. Second, we *quantify* the relative gains of three different levels of RF-environment awareness and study the impact of indoor shadowing on their associated joint network capacity region. We show that capacity tradeoffs between primary and secondary networks depend on white space detection technique, resulting in joint network capacity regions which range from complement convex to linear to (almost) convex, see e.g., Fig.1. Not surprisingly the signal energy detection approach's network capacity region is the smallest, but, perhaps surprisingly, secondary network's capacity exhibits a non-monotonic behavior in the attenuation associated with indoor shadowing. By contrast when secondary nodes use positioning assisted and receiver location-aware techniques substantial gains in capacity can be realized, and their capacity increases *monotonically* as indoor shadowing increases. A final key observation quantified in this paper is how the capacity gain of knowing primary receivers locations versus simply knowing the position of primary transmitters, varies with the density of primary receivers. This suggests that when a system has a high density of primary receivers, such detailed information may not be worthwhile, i.e., simpler cognitive mechanisms may suffice.

Organization This paper is organized as follows. In Section II, we provide a detailed description of our model, white space detection techniques, and definitions of the relevant system parameters. In Section III, evaluation methodology is explained with overview of results. In Sections IV to VI, the outage probabilities of primary and secondary receivers

under three different sensing techniques are computed. These outage probabilities are used to find the maximum contention densities of STxs under an outage constraint in Section VII. In Section VIII, we define the capacity of primary and secondary networks and combine them to compute a joint network capacity region. Section IX concludes the paper.

II. System Model

A. Indoor Shadowing, Pathloss, and Interference Model

In order to understand the impact of complex heterogenous environments on cognitive network capacity we shall model a network where indoor and outdoor nodes coexist. Signals propagating from the inside to the outside, and vice versa, see, for simplicity, a *fixed* attenuation ψ, where $0 \leq \psi \leq 1$, due to building walls. We refer to this as a indoor shadowing level. In practice such losses are highly dependent on a building's construction materials - measurements suggest variations from -40dB to 0dB [25]. Propagation in the environment is captured using a simple free space pathloss model. That is, if both the transmitter and receiver are outdoors, or both within the same building, then, the attenuation factor is $d^{-\alpha}$, where d is the distance from the transmitter to the receiver, and α is the pathloss attenuation factor. If one of them is outdoors while the other indoors, then the signal is attenuated by an additional factor ψ associated with the traversing building walls. If the transmitter and receiver are indoor but in different buildings, then, a further additional factor of ψ is introduced, giving a total attenuation of $\psi^2 d^{-\alpha}$. Such a model could be made richer by considering different path loss attenuations in indoors and outdoors as well as variable indoor shadowing, yet as we will see in the sequel, analysis is already quite complex, and perhaps to first order it suffices towards understanding the role of heterogeneity in the network environment.

Throughout the paper, the signal to interference plus noise ratio (SINR) at a receiver, is computed based only on the dominant interferer, i.e., that which contributes the most interference, and a fixed SINR decoding threshold. Thus an outage corresponds to having at least one interfering node within a given disc of a fixed radius centered at the receiver. The *interference radius* of a receiver depends on various parameters including the ambient noise power, interferer's transmit power, receiver's received signal power and the decoding threshold. This will be discussed in more detail in Section II-E.

B. Primary Network

We shall assume the locations of active primary transmitters (PTx) follow a Poisson point process (PPP) $\Pi_p = \{X_j\}$ with intensity λ_p on $\mathbf{R}^2$. Here X_j denotes both j-th PTx as well as its location. A PTx X_j uses a transmit power ρ_p and covers a region $b(X_j, d_p)$, where $b(x, r)$ denotes a disc centered at x with radius r and d_p is the coverage radius of a PTx. A primary receiver (PRx) located within the PTxs' coverage area $B(\Pi_p, d_p) \equiv \cup_{X_j \in \Pi_p} b(X_j, d_p)$, is assumed to successfully receive the primary signal as long as it does not see secondary interferers. We let β_p denote the decoding SINR for PTx's signal and $b_p = \log(1 + \beta_p)$ be the transmission rate of PTxs. The locations Π_r of PRxs are assumed to follow a homogenous PPP conditioned on the coverage area of the PTxs, thus this is a stationary doubly stochastic process (or Cox process) with a random intensity measure given by $\lambda_r \mathbf{1}\{z \in B(\Pi_p, d_p)\}$ at location $z \in \mathbf{R}^2$, where $\mathbf{1}\{\}$ denotes the indicator function, see [26]. A PRx Y is interfered by STxs if there is at least one secondary transmitter (STx) in $b(Y, r_{sp})$, where r_{sp} is the interference radius of a PRx with respect to a STx, determined in Section II-E. We assume that all PTxs and PRxs are outdoors[2]. This is a worst case scenario since indoor PRxs, if any, are better protected from interference. We refer to (Π_p, Π_r) as the primary network.

C. Secondary Network

The locations of STxs are also modeled as a PPP Π_s on $\mathbf{R}^2$ but with intensity λ_s. The locations of indoor secondary transmitters (iSTx) Π_{si} are obtained by independent thinning of Π_s with probability a_i. The remaining STxs Π_{so} correspond to outdoor secondary transmitters (oSTx). Thus Π_{si} and Π_{so} are PPP with intensities $\lambda_{si} \equiv a_i \lambda_s$ and $\lambda_{so} \equiv a_o \lambda_s$ respectively, where $a_o = 1 - a_i$.

We assume STxs use a cognitive function to detect white space and then contend with each other using a simple ALOHA protocol, as done in [12], [27], [28]. STxs transmit at power ρ_s. Not all STxs in Π_{si} and Π_{so} are active, so we will introduce additional processes to denote active STxs. These are once again Cox processes with non homogenous intensity given the locations of the primary network $\{\Pi_p, \Pi_r\}$. Specifically, the intensity of active iSTxs at location z given $\{\Pi_p, \Pi_r\}$ is given by

$$a_i \lambda_s \mathbf{1}\{\text{iSTx at } z \text{ is active under } \{\Pi_p, \Pi_r\}\}$$

where the indicator function depends on a the white space detection technique being considered. Techniques, for determining the transmission opportunities for STxs, will be explained the next section. We assume each STx has an associated secondary receiver (SRx) randomly located at a fixed distance d_s and both are either indoor or outdoors. [3] Note that SRxs can be interfered by unintended STxs or PTxs. More specifically, an outage may occur at oSRx W_o if there are one or more oSTxs within $b(W_o, r_{ss}^{oo})$; or if, there are one or more iSTxs in $b(W_o, r_{ss}^{io})$, where r_{ss}^{oo} and r_{ss}^{io} are the interference radii of a oSRx with respect to oSTxs and iSTxs respectively. In general $r_{ss}^{oo} \geq r_{ss}^{io}$ since iSTx will offer less interference to oSRx due to penetration loss ψ. Similarly an iSRx W_i can be interfered by either oSTxs in $b(W_i, r_{ss}^{oi})$ or iSTxs in $b(W_o, r_{ss}^{ii})$, where r_{ss}^{oi} and r_{ss}^{ii} are the interference radii of a iSRx with respect to a oSTx and iSTx respectively. Generally $r_{ss}^{oi} \geq r_{ss}^{ii}$ holds since iSTx gives less interference to iSRx due to the strong penetration loss ψ^2. An oSRx W_o is interfered by PTxs if there exist any PTx in $b(W_o, r_{ps})$, where

[2] In real world, some PRxs are indoors. However, we only consider outdoor PRxs in this paper since assuming some portion of PRxs are indoors has almost no impact on our results. This is because the operations or parameters of secondary nodes are determined based on/considering only the performance of outdoor PRxs that are in worse condition than indoor PRxs in terms of robustness to interference.

[3] By assuming fixed distance d_s between STx and SRx, we do worst case analysis.

r_{ps} is the interference radius of oSRx with respect to a PTx. Similarly, a iSRx W_i can be interfered by PTxs if there exist any PTx in $b\left(W_i, r_{ps}^i\right)$, where r_{ps}^i is the interference radius of a iSRx with respect to a PTx. We assume that STxs transmit with rate $b_s = \log\left(1+\beta_s\right)$ where β_s is the decoding SINR threshold for STx's signal. The various parameters introduced here will be specified in Section II-E.

D. White Space Detection

Three different methods are considered for detecting transmission opportunities for secondary nodes. They are neither the worst nor the best, but rather represent the spectrum of possible approaches exploiting different levels of RF-environment awareness that STxs could have of the surrounding environment. Note that in [15] FCC requires cognitive devices to have both signal energy detection scheme and geo-location/data base access scheme that corresponds to the first and second methods in our work. Cognitive devices relying only on the signal energy detection method can be allowed to be used but should pass FCC's much more rigorous test.

Signal Energy Detection Based Cognitive Devices. Signal energy detection is a simple technique which relies on measuring the PTxs' signal energy at a STx's location. If it is below a predetermined detection threshold, the STx infers that there is no PTx in its detection – again modeled as a disc centered at the STx and a given detection radius. Increasing the threshold makes the STx only sensitive to PTxs which are close by, i.e., the detection radius is a strictly decreasing function of the threshold. Decreasing the threshold makes the detector more sensitive, and accordingly the STx will behave conservatively. Although this approach appears reasonable it has a serious weakness. A STx which is indoors will see an attenuated signal from outdoor PTxs, and may conclude there are no nearby PTxs, and transmit within coverage area of PTxs possibly producing harmful interference to PRxs. To preclude from this happening, the detection threshold needs to be set very conservatively. This point will be discussed further in Section IV-A where we will quantify the impact of iSTxs on PRx's outage probability. In the sequel we let E-STx(E-SRx) denote STx(SRx) using the signal energy detection method. When we need to be more specific on node's location, i.e., indoor or outdoor, we use E-iSTx(E-iSRx) and E-oSTx(E-oSRx) for an indoor and an outdoor E-STx(E-SRx) node respectively.

Positioning-assisted Cognitive Devices. A STx using positioning-assisted detection is aware of the actual locations of nearby PTxs. We assume that either the device has preloaded map in its memory or it can access remote database. The device periodically samples its current location using its built-in positioning module and checks if it is safe to transmit or not. We assume that when STxs are outdoors they use Global Positioning System(GPS) technology and when they are indoors they use indoor positioning technology [29] or infer its location information based on previous history of location information. Two similar ideas were discussed in [20], [21]. A cognitive device using this approach knows the coverage area of PTxs, and so does not have the drawback of mis-detecting PTxs discussed for the previous method. It allows both indoor and outdoor STxs to correctly detect the presence of PTxs or equivalently the regions where STxs are not allowed to transmit. In fact, this approach is equivalent to a technique letting a cognitive device know whether it is indoors or outdoors. The device using the information can adaptively adjust its signal energy detection threshold so as to protect primary receivers and to maximize its transmission opportunity. We shall use a similar naming convention, where G-STx(G-SRx), G-iSTx(G-iSRx) and G-oSTx(G-oSRx) denote a positioning-assisted STx(SRx), a positioning-assisted indoor STx(SRxs), and a positioning-assisted outdoor STx(SRx) respectively.

Receiver Location-Aware Cognitive Devices. Lastly suppose cognitive devices can detect the locations of both PTxs and PRxs. Whether this is implementable depends on the nature of PRxs. If the PRxs are passive it may not be easy to detect them. However, even in this case, it may not be totally impossible if one can detect the leakage power of receiver's oscillator, see [22]. [30] shows that this kind of detecting scheme is implementable and have been used in the UK to find people watching TV without buying licenses. If PRxs can send a signal (beacon) to indicate their existence to nearby STxs, then, it is of course much easier to detect and protect them. Alternatively the location of PRxs to be protected could be registered in a database accessible by STxs. We shall thus suppose STxs are able to detect the presence of PRxs within a certain radius. This affords cognitive devices the highest degree of RF-environment awareness. STxs can now transmit within the coverage of PTxs[4] as long as they do not give harmful interference to PRxs (or equivalently there are no PRxs close to them). We again adopt a naming convention, where L-STx(L-SRx), L-iSTx(L-iSRx) and L-oSTx(L-oSRx) denote a receiver location-aware STx(SRx), a receiver location-aware indoor STx(SRx), and a receiver location-aware outdoor STx(SRx) respectively.

E. System Model Parameters

Below we derive many of the above mentioned model parameters, from those specified as a part of system design and requirements, e.g., ρ_p, ρ_s, β_p and β_s. We let i_p denote the maximum tolerable interference at the edge of PTx's coverage area. i_p is a design parameter that corresponds to a performance margin which makes receivers robust to a certain amount of interference, so we assume this value is given and fixed. This, and the successful reception condition for PRx, determine the coverage range d_p of a PTx. That is, under maximum interference, the received SINR of a PRx at distance d where $d < d_p$ from its nearest PTx should be larger than the decoding SINR threshold β_p, which defines the coverage range of a PTx as

$$d_p \equiv \sup\left\{d>0 | \frac{\rho_p d^{-\alpha}}{\eta + i_p} > \beta_p\right\} = \left(\frac{\rho_p}{(\eta+i_p)\beta_p}\right)^{\frac{1}{\alpha}},$$

[4]According to the current rule by FCC, cognitive devices are not allowed to operate inside the coverage of primary transmitter. But, in this paper, by allowing it we study how much capacity improvement we can expect if we can overcome the current limitation.

where η denotes the noise power. By considering i_p in computing d_p, we do a worst case analysis.

Next we determine the smallest allowable distance $r_{sp}(d)$ between an oSTx and a PRx, given the latter is a distance d from its nearest PTx. Ensuring successful reception means that:

$$r_{sp}(d) \equiv \inf\left\{r>0|\frac{\rho_p d^{-\alpha}}{\eta+\rho_s r^{-\alpha}}>\beta_p\right\} = \rho_s^{\frac{1}{\alpha}}\left(\frac{\rho_p}{d^\alpha\beta_p}-\eta\right)^{-\frac{1}{\alpha}}. \quad (1)$$

We will call $r_{sp}(d)$ the *PRx's interference radius with respect to an oSTx*. The *PRx's interference radius with respect to an iSTx* is similarly given by

$$r^i_{sp}(d) \equiv \inf\left\{r>0|\frac{\rho_p d^{-\alpha}}{\eta+\psi\rho_s r^{-\alpha}}>\beta_p\right\} = \psi^{\frac{1}{\alpha}} r_{sp}(d).$$

Note that $r_{sp}(d)$ and $r^i_{sp}(d)$ are strictly increasing functions of d. Indeed, as the PRx gets further away from its nearest PTx, the PRx is increasingly vulnerable to interference, and so the above radii increase. In the sequel we will occasionally omit the dependency of r_{sp} and r^i_{sp} on d.

Next we determine the maximum tolerable interference of a SRx i_s. A SRx a distance d_s away from its STx can decode the signal from the STx, if the received SINR is larger than β_s; this gives the following requirement

$$i_s \equiv \sup\left\{i>0|\frac{\rho_s d_s^{-\alpha}}{\eta+i}>\beta_s\right\} = \frac{\rho_s d_s^{-\alpha}}{\beta_s}-\eta. \quad (2)$$

In turn an *oSRx's interference radius w.r.t. a PTx*, r_{ps} can be determined by ensuring the interference from its nearest PTx does not exceed i_s, i.e.,

$$r_{ps} \equiv \inf\left\{r>0|\rho_p r^{-\alpha}+\eta\le i_s\right\} = \left(\frac{\rho_p}{i_s-\eta}\right)^{\frac{1}{\alpha}}. \quad (3)$$

Similarly, the *iSRx's interference radius w.r.t. a PTx* r^i_{ps} follows by including the additional indoor shadowing level ψ that the indoor SRx would see:

$$r^i_{ps} \equiv \inf\left\{r>0|\psi\rho_p r^{-\alpha}+\eta\le i_s\right\} = \psi^{\frac{1}{\alpha}} r_{ps}. \quad (4)$$

There are four different types of SRx's interference radii related to STxs. The *oSRx's interference radius w.r.t. an oSTx* r^{oo}_{ss} is computed as follows. For an oSRx to receive its oSTx's signal without outage, the noise plus interference from its nearest interfering oSTx to the oSRx should not exceed the tolerable interference $\rho_s r^{-\alpha}+\eta\le i_s$, giving

$$r^{oo}_{ss} \equiv \inf\left\{r>0|\rho_s r^{-\alpha}+\eta\le i_s\right\} = \left(\frac{\rho_s}{i_s-\eta}\right)^{\frac{1}{\alpha}}.$$

The *oSRx's interference radius w.r.t. an iSTx* r^{io}_{ss} is determined by the interference condition $\psi\rho_s r^{-\alpha}+\eta\le i_s$, which gives

$$r^{io}_{ss} \equiv \inf\left\{r>0|\psi\rho_s r^{-\alpha}+\eta\le i_s\right\} = \psi^{\frac{1}{\alpha}} r^{oo}_{ss}.$$

The *iSRx's interference radius w.r.t. an oSTx* r^{oi}_{ss} is determined by the interference condition $\psi\rho_s r^{-\alpha}+\eta\le i_s$, giving

$$r^{oi}_{ss} \equiv \inf\left\{r>0|\psi\rho_s r^{-\alpha}+\eta< i_s\right\} = \psi^{\frac{1}{\alpha}} r^{oo}_{ss}.$$

The *iSRx's interference radius w.r.t. an iSTx* in a different building r^{ii}_{ss} is determined by the interference condition $\psi^2\rho_s r^{-\alpha}+\eta\le i_s$, giving

$$r^{ii}_{ss} \equiv \inf\left\{r>0|\psi^2\rho_s r^{-\alpha}+\eta\le i_s\right\} = \psi^{\frac{2}{\alpha}} r^{oo}_{ss}.$$

ρ_p	Transmit power of PTx
ρ_s	Transmit power of STx
β_p	Decoding SINR of PRx
β_s	Decoding SINR of SRx
d_p	Coverage range radius of PTx
i_p	Maximum tolerable interference of PRx at the edge of PTx coverage
i_s	Max tolerable interference of a SRx at distance d_s from its STx
r^{E}_d	Detection radius of E-oSTx
r^{L}_d	Detection radius of L-oSTx
r_{ps}	Interference radius of oSRx w.r.t. PTx
r^i_{ps}	Interference radius of iSRx w.r.t. PTx
r^{oo}_{ss}	Interference radius of oSRx w.r.t. oSTx
r^{io}_{ss}	Interference radius of oSRx w.r.t. iSTx
r^{oi}_{ss}	Interference radius of iSRx w.r.t. oSTx
r^{ii}_{ss}	Interference radius of iSRx w.r.t. iSTx
r_d	Detection radius (baseline)
$r_{sp}(d)$	Interference radius of a PRx w.r.t. to oSTx
$r^i_{sp}(d)$	Interference radius of a PRx w.r.t. to iSTx
$r^{\mathrm{E}i}_d$	Detection radius of E-iSTx
$r^{\mathrm{L}i}_d$	Detection radius of L-iSTx
α	Pathloss attenuation factor
a_i	Fraction of indoor STxs
a_o	Fraction of outdoor STxs $(=1-a_i)$
λ_s	Density of STxs
ψ	Indoor shadowing level
λ_p	Density of PTxs
η	Noise power

TABLE I: Summary of Parameters

A STx using *signal energy detection*, E-STx, ensures there are no PTxs close by, i.e., within its *detection radius* r_d, so as to indirectly protect PRxs. The baseline detection radius used for E-oSTx is defined as

$$r_d \equiv \max\left\{d_p + r_{sp}(d_p), d_s + r_{ps}\right\}. \quad (5)$$

The first term in the maximum ensures that the STx is far enough so as to not harm PRx which is at the edge, i.e., a distance d_p, from its associated PTx. Thus STx's can send only if they are outside the PTxs' coverage area plus an additional guard zone. The second term corresponds to minimum distance a SRx must be from a PTx, r_{ps} plus the SRx's fixed distance d_s from its associated STx. If the secondary network includes indoor STx then protecting PRxs requires increasing the detection radius to $r^{\mathrm{E}}_d \equiv \psi^{-\frac{1}{\alpha}} r_d$, We discuss this in more detail in the sequel along with modeling of detection radii for the two other white space detection methods to be considered.

F. Preliminary Definitions

In this section, we define some further notations used throughout the paper. Let $|\mathcal{A}|$ denote the area of a set $\mathcal{A}\subset\mathbf{R}^2$.

Let $\|x-y\|$ denote the distance between x and y in $\mathbf{R}^2$. We define a set $K(x,r_x;y,r_y) \equiv b(y,r_y)\setminus b(x,r_x)$ in $\mathbf{R}^2$. Let $\mathcal{L}_{\{Q\}}(\lambda_s) \equiv \mathbb{E}\left[e^{-\lambda_s Q}\right]$ be the Laplace transform of a random variable Q. For simplicity we let $q_m^{oo} = \pi\left(r_{ss}^{oo}\right)^2$, $q_m^{io} = \pi\left(r_{ss}^{io}\right)^2$, $q_m^{oi} = \pi\left(r_{ss}^{oi}\right)^2$, $q_m^{ii} = \pi\left(r_{ss}^{ii}\right)^2$, $q_m^{o} = a_i q_m^{io} + a_o q_m^{oo}$ and $q_m^{i} = a_i q_m^{ii} + a_o q_m^{io}$. For a given $x \in \mathbf{R}^2$ and PPP Π, $x \notin B(\Pi, r)$ and $\Pi \cap b(x,r) = \emptyset$ will denote the same event.

G. Parameter Set

Throughout the paper, we use the following representative parameters to compute the system model parameters defined in Section II-E: $\alpha = 3$, $\eta = N_o \times 20 \times 10^6$, $i_p = 5\eta$, $\rho_p = 100$W, $\rho_s = 1$mW, $\beta_p = 10$, $\beta_s = 1.4$, where $N_o = -174$dBm is an noise power spectral density. Some of the resulting computed system parameters are as follows: $d_p = 27560$m, $i_s = 7.14 \times 10^{-7}$, $d_s = 10$m, $r_{ps} = 519$m, and $r_{ss}^{oo} = 11.18$m. See [16], [31], [32] for some realistic parameter values. and [33] for parameter selection.

H. Weaknesses of Model

Our model has several weaknesses. First, our channel model accounts for pathloss attenuation and indoor/outdoor shadowing factor only. Fading is not considered. Second, our interference model does not account for the additive nature of interference. Indeed as mentioned earlier, we assume that outages are caused solely by the dominant interferer. This choice is driven mathematical simplicity, yet for spatially distributed nodes, this has been proven as a fairly good model [6], [34], [35]. Moreover, it turns out that outage probability computed with this simple disk model corresponds to the lower bound of outage computed considering shot noise interference, and it has been shown that the lower bound is asymptotically tight, see [12], [28]. Third, the location of primary transmitters is modeled as PPP. Clearly this is not likely to be true in practice for any type of designed infrastructure. Still this provides a simple caricature of the spatial variability one might see in such deployments. Finally, we assume STxs transmit in Aloha fashion, this again is assumed for tractability, following [12], [27], [28], [36]. Some of our results could perhaps be extended to account for clustering in PTxs and/or STxs, yet via a non-homogenous point process but from now it seems reasonable to focus on understanding the homogenous case.

III. Computing joint Network capacity Region Roadmap and Overview of Results

A. Computing a Joint Network Capacity Region Roadmap

Our goal is to compare the *joint network capacity region* $\Lambda = \{(C_1,C_2)|(C_1,C_2)$ are achievable$\}$, i.e., the set of achievable primary and secondary capacity pairs (C_1,C_2), under the three white space detection techniques. The notion of joint network capacity region studied in this paper is *different* from the classical one in information theory [37] in at least three ways. First, a primary network's *broadcast coverage capacity* C_1 is defined as the average number of bits that can be successfully received by potential receivers per second per square meter per Hertz. Since the primary network operates in the broadcast mode this is simply proportional to transmission rate b_p times the fraction of covered area. The covered area depends on the density of primary transmitters λ_p and potentially also on secondary nodes' behavior if it fails to protect the primary network. Second, the secondary network's *transmission capacity* C_2 is the average number of successfully transmitted bits per second per square meter per Hertz subject to an ϵ-outage constraint summed over indoor and outdoor transmissions. This is similar to the notion introduced in [12], [27], except that in a cognitive network context, the secondary nodes' transmission capacity depends on the density of primary nodes, fractions of indoor/outdoor secondary nodes, the environment, e.g., path loss and indoor shadowing as well as the white space detection technique being used. Third, a pair (C_1,C_2) is "achievable" if there exists a density of primary and secondary nodes such that the average spatial capacity of both the primary and secondary network is (C_1,C_2). Note that C_1 and C_2 correspond to averages computed over an ensemble of Poisson distributed primary and secondary nodes under our system models. The mathematical definition of the joint network capacity region will be given in Section VIII.

The computation of the joint network capacity region involves three steps. First determining the outage probabilities for primary and secondary (indoor/outdoor) nodes. This is carried out for each white space detection technique in Sections IV–VI. Second, for a fixed intensity of primaries nodes λ_p determining the optimal intensity of secondary transmissions λ_s^ϵ which meets the outage constraint ϵ, see Section VII. Third, computing the joint network capacity region by varying the possible intensity of primary nodes see in Section VIII. Prior to doing so, we discuss some of the key obtained results.

B. Overview of Results

Fig.1 exhibits representative joint network capacity regions for the cognitive network under the three white space detection mechanisms considered, while Fig.2 exhibits the geometry underlying these results. As expected the capacity is enhanced when secondary nodes have a higher degree of RF-environment awareness.

In the signal energy sensing scenario the detection radius must be set conservatively because indoor STx can not properly infer the location of PTxs and thus protect PRxs. As shown in Fig.2a E-oSTx nodes can only operate if they are outside this larger radius r_d^{E}, while because of the indoor shadowing E-iSTx can operate outside the ('correct') radius r_d. As exhibited in Fig.1 the joint network capacity region for this scenario is surprisingly complement convex. Note it is tempting to think time sharing would convexify the network capacity region, yet this does not make sense in the scenario of interest, i.e., where a pre-installed broadcasting network's licensed spectrum is being opportunistically used by an ad hoc cognitive network.

The positioning-assisted white space detection technique solves this problem since all G-STxs are made directly aware of the coverage area of PTxs. Fig.2b shows a typical realization of the two networks, where both G-iSTxs and G-oSTx can

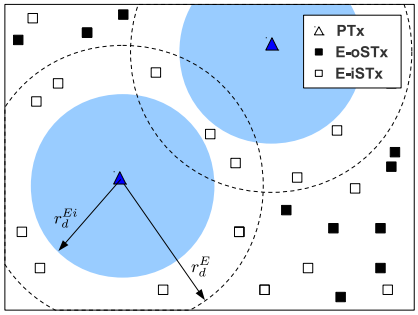

(a) Signal energy detection method: indoor environment causes interference attenuation, which makes E-iSTxs feel attenuated interference power. Thus, conservative(large) detection radius r_d^{E} is required.

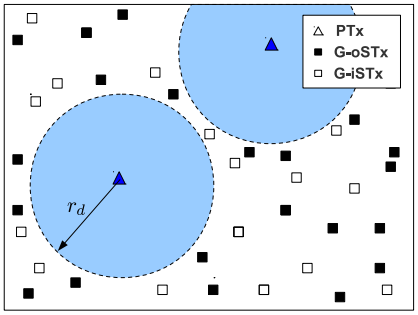

(b) Positioning-assisted method: both G-iSTx and G-oSTx have the same detection radius r_d, which allow them fully utilize white space.

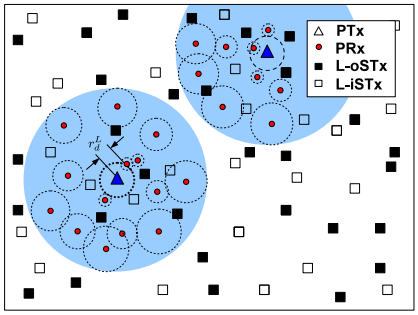

(c) Receiver location-aware method: as long as not giving interference to PRxs, L-STxs can operate even inside the coverage of PTxs. L-STxs are not allowed to transmit inside the PRx's interference region (circle around each PRx).

Fig. 2: A typical realization of primary and secondary networks under three white space detection methods is shown. Shaded region denotes the coverage of PTxs with radius d_p.

operate outside coverage area of PTxs. The joint network capacity region is shown to be roughly linear in this case, see Fig.1.

Last, if STxs are aware of primary receivers' locations one obtains substantial capacity improvements. Indeed, depending on the locations of PRxs, L-STxs can opportunistically transmit *within* the coverage area of PTxs, so the capacity gains now depend on the density of primary receivers, see Fig.1. Fig.2c, exhibits the geometry underlying this scenario. The small discs around each PRx denote its interference region w.r.t. a L-oSTx[5]. To protect PRxs no L-oSTx should reside in such discs. The radii of these discs are defined in (1) as $r_{sp}(d)$ which is strictly increasing function of distance d to its nearest PTx. Perhaps counterintuitively, L-STxs located closer to PTxs are more likely to transmit than L-STxs far from them. Also surprisingly, it turns out that this phenomenon is helpful in increasing secondary capacity when λ_p is high, this can be seen in Fig.1, where the receiver location aware capacity region for $\lambda_r = 10^{-4}$ exhibits a non monotonic behavior on the right hand side.

IV. Performance of Signal Energy Detection Technique

In this section, we evaluate the outage probability of a PRx and E-oSRx. We will first show that if an indoor STx chose its detection radius r_d (or equivalently detection threshold) naively, this can negatively impact PRxs. For notational simplicity, let Π'_{so} and Π'_{si} be Cox processes denoting active (or transmitting) E-oSTxs and E-iSTxs with intensities $a_o\lambda_s\mathbf{1}\left\{z \notin B\left(\Pi_p, r_d\right)\right\}$ and $a_i\lambda_s\mathbf{1}\left\{z \notin B\left(\Pi_p, r_d^i\right)\right\}$ at $z \in \mathbf{R}^2$ respectively and, where $r_d^i \equiv \psi^{\frac{1}{\alpha}} r_d$.

A. Outage Probability of Primary Receivers

Suppose we set the detection threshold, say I_d, of E-STxs such that $\rho_p r^{-\alpha} > I_d$ for $r < r_d$. Then, E-oSTxs would detect any PTxs within r_d and would not interfere PRxs that are at the edge of the PTxs' coverage area. However, E-iSTx can only detect PTxs within r_d^i, which potentially makes them mis-detect PTxs between r_d^i and r_d. To show the negative impact of this parameter choice, we shall compute the outage probability of a PRx as a function of distance d to its nearest PTx.

Theorem 1. *(Conditional Outage Probability of PRx with E-STxs) For given λ_p, λ_s, and d_p, a PRx Y's outage probability given it is a distance d away from its nearest PTx X is given by*

$$P_{out}^p(d,\lambda_s) = 1 - \mathbf{1}\{d < d_p\}\mathcal{L}_{\{a_o L_1(d,\Pi_p^{(2)}) + a_i L_2(d,\Pi_p^{(2)})\}}(\lambda_s), \tag{6}$$

where $\Pi_p^{(2)} = \{\Pi_p \cap \overline{b(Y,d)}\} \cup \{X\}$,
$L_1(d,\Pi) = \int_{K(X,r_d;Y,r_{sp})} \mathbf{1}\{z \notin B(\Pi, r_d)\}\, dz$, *and*
$L_2(d,\Pi) = \int_{K(X,r_d^i;Y,r_{sp}^i)} \mathbf{1}\{z \notin B\left(\Pi, r_d^i\right)\} dz$.

Proof is given in Appendix A. Note that geometrically $L_1(d,\Pi_p^{(2)}) = \int_{K(X,r_d;Y,r_{sp})} \mathbf{1}\{z \notin B(\Pi^{(2)}, r_d)\} dz$ is an area of $K(X, r_d; Y, r_{sp})$ which is not covered by the Boolean process $B\left(\Pi^{(2)}, r_d\right)$ and a similar interpretation applies to $L_2(d,\Pi_p^{(2)})$. $L_1(d,\Pi_p^{(2)})$ can be viewed as a random variable with finite support since it depends on the random process $\Pi_p^{(2)}$. Note that this area measures the amount of potential interferers. Thus, a larger area implies that the PRx Y is more likely to be interfered with. To compute the above Laplace transform $\mathcal{L}_{\{a_o L_1(d,\Pi_p^{(2)}) + a_i L_2(d,\Pi_p^{(2)})\}}(\lambda_s)$, we need to know the distributions of two random variables $L_1(d,\Pi_p^{(2)})$ and $L_2(d,\Pi_p^{(2)})$, but these are difficult to compute. So, we will compute upper and lower bounds on these quantities. Here we shall use the following result to compute bounds of the transform of such non-negative random variables, it follows from simple results on convex ordering for random variables. Proof is given in [38].

Lemma 2. *(Bounding non-negative random variables) Suppose X is a random variable with bounded support $[0,p]$ and mean $\mathbb{E}[X]$. Then, $\mathbb{E}[\phi(X)] \leq \phi(0) - \frac{\mathbb{E}[X]}{p}(\phi(0) - \phi(p))$ for all convex function ϕ.*

[5]We can also draw its interference region w.r.t. a L-iSTx, but it is omitted for simplicity.

The following corollary gives lower bounds on $P_{out}^{p}(d)$ obtained using Lemma 2, while the upper bound is obtained using Jensen's inequality.

Corollary 3. *For $d < d_p$, upper and lower bounds of a PRx's conditional outage probability are given by:*

$$P_{out}^{p,u}(d,\lambda_s) = 1 - \exp\{-\lambda_s(a_o l_1 + a_i l_2)\}, \text{ and}$$
$$P_{out}^{p,l}(d,\lambda_s) = \frac{a_o l_1 + a_i l_2}{a_o l_{1m} + a_i l_{2m}}(1 - e^{-\lambda_s(a_o l_{1m} + a_i l_{2m})}),$$

where $l_1 = \mathbb{E}[L_1(d,\Pi_p^{(2)})]$, $l_2 = \mathbb{E}[L_2(d,\Pi_p^{(2)})]$, $l_{1m} = |K(X,r_d;Y,r_{sp})|$ and $l_{2m} = |K(X,r_d^i;Y,r_{sp}^i)|$.

In the sequel, we omit proofs of remaining corollaries giving such bounds since all of them can be proved using the same machinery. Note that $l_1 = \mathbb{E}[L_1(d,\Pi_p^{(2)})]$ and $l_2 = \mathbb{E}[L_2(d,\Pi_p^{(2)})]$ can be computed through numerical integration as follows:

$$\begin{aligned} l_1 &= \int_{K(X,r_d;Y,r_{sp})} P(z \notin B(\Pi_p^{(2)}, r_d))dz \\ &= \int_{K(X,r_d;Y,r_{sp})} \exp\{-\lambda_p |K(X,d;z,r_d)|\}dz, \\ l_2 &= \int_{K(X,r_d;Y,r_{sp}^i)} P(z \notin B(\Pi_p^{(2)}, r_d^i))dz \\ &= \int_{K(X,r_d;Y,r_{sp}^i)} \exp\{-\lambda_p |K(X,d;z,r_d^i)|\}dz. \end{aligned}$$

Fig.3a shows the outage probability of a PRx as a function of d to its nearest PTx when $a_o = 1$, i.e., when there are no E-iSTx. One PTx at the origin is considered. In this case, we have a coverage $d_p = 27559$m, and the detection radius r_d is set to $d_p + r_{sp}(d_p)$ after considering guard band of width $r_{sp}(d_p)$. As expected, the outage probability is zero for $d < d_p$ and non-zero otherwise. However if there exist indoor nodes (i.e., $a_i > 0$) with $\psi = -10$dB, we have a significant increase in the outage probability as shown in Fig.3b. Since $r_d^i < r_d$, the attenuated signal from the PTx makes E-iSTxs between r_d^i and r_d mis-detect the PTx and allows them to transmit even inside the coverage area of the PTx. This becomes increasingly severe if ψ gets stronger(or smaller). These two figures clearly show how poorly selected detection radii of STxs can give harmful interference to PRxs. To prevent this, one has to set the detection threshold *conservatively* so that all the E-iSTxs at $d < d_p$ detect the PTx. We reconsider the outage probability calculation under a more conservative detection radius choice in next section.

B. Outage Probability for Primary Receiver with STxs using a Conservative Detection Threshold

In order to properly protect PRxs in the coverage area of PTxs, we shall make all STxs use the detection radius $r_d^{\mathrm{E}} \equiv \psi^{-\frac{1}{\alpha}} r_d$, where r_d is the desired minimum detection radius defined in (5). Note that E-oSTxs using r_d^{E} can detect all PTxs in their detection radius r_d^{E}, but E-iSTxs using r_d^{E} only detect PTxs in an effective detection radius of $\psi^{\frac{1}{\alpha}} r_d^{\mathrm{E}} = r_d$ since E-iSTxs are indoor and see attenuated PTx power. They see the PTxs' appear further away than their actual locations. So, considering this effect, E-STxs must use a conservative detection radius r_d^{E}.

Accordingly, let Π_{so}^{E} and Π_{si}^{E} be Cox processes denoting active E-oSTxs and E-iSTxs that would arise given these new detection radii with intensities $a_o\lambda_s \mathbf{1}\left\{z \notin B\left(\Pi_p, r_d^{\mathrm{E}}\right)\right\}$ and $a_i\lambda_s \mathbf{1}\left\{z \notin B\left(\Pi_p, r_d^{\mathrm{E}i}\right)\right\}$ at $z \in \mathbf{R}^2$ respectively. Note that E-STxs no longer transmit inside the coverage area of the PTxs due to this new detection threshold. However, as a side effect this will make E-oSTx less likely to be active since they need to detect a larger PTx free area to be active. We update Theorem 1 and Corollary 3 by replacing r_d with r_d^{E} and r_d^i with $r_d^{\mathrm{E}i} \equiv \psi^{\frac{1}{\alpha}} r_d^{\mathrm{E}}$, to obtain Theorem 4 and Corollary 5 respectively. Fig.8b shows the updated results from Fig.8a. Note that due to conservative detection radius there are no E-STxs inside $b(X, r_d)$ that can harm PRxs.

Theorem 4. *(Outage Probability of PRx with E-STxs with conservative detection radius) For a PRx Y at a distance d from its nearest PTx, we have an outage probability*

$$P_{out}^{p\mathrm{E}}(d,\lambda_s) = 1 - \mathbf{1}\{d < d_p\}\mathcal{L}_{\{a_o L_3(d,\Pi_p^{(2)}) + a_i L_4(d,\Pi_p^{(2)})\}}(\lambda_s)$$

where $L_3(d,\Pi) = \int_{K(X,r_d^E;Y,r_{sp})} \mathbf{1}\{z \notin B(\Pi, r_d^{\mathrm{E}})\}dz$, and $L_4(d,\Pi) = \int_{K(X,r_d^{Ei};Y,r_{sp}^i)} \mathbf{1}\{z \notin B(\Pi, r_d^{\mathrm{E}i})\}dz$.

This outage probability can be upper and lower bounded as follows.

Corollary 5. *For $d < d_p$, upper and lower bounds on a PRx's conditional outage probability are given by:*

$$P_{out}^{p\mathrm{E},u}(d,\lambda_s) = 1 - \exp\{-\lambda_s(a_o l_3 + a_i l_4)\} \quad \text{and}$$
$$P_{out}^{p\mathrm{E},l}(d,\lambda_s) = \frac{a_o l_3 + a_i l_4}{a_o l_{3m} + a_i l_{4m}}(1 - e^{-\lambda_s(a_o l_{3m} + a_i l_{4m})}),$$

where $l_3 = \mathbb{E}[L_3(d,\Pi_p^{(2)})]$, $l_4 = \mathbb{E}[L_4(d,\Pi_p^{(2)})]$, $l_{3m} = \left|K(X,r_d^{\mathrm{E}};Y,r_{sp})\right|$ and $l_{4m} = \left|K(X,r_d^{\mathrm{E}i};Y,r_{sp}^i)\right|$.

Again l_3 and l_4 can be computed numerically, see [38]. The outage probability of a PRx with E-STxs having conservative detection radius r_d^{E} is the same as that in Fig.3a. Due to the increased detection radius, now PRxs are free from interference from E-STxs.

Next we compute the fraction of area of $\mathbf{R}^2$ where potential PRxs can successfully receive PTxs' transmission $P_c^{\mathrm{E}}(\lambda_p) = 1 - \mathbb{E}[P_{out}^{p\mathrm{E}}(D,\lambda_s)]$. Note that primary network's broadcasting coverage capacity is directly proportional to this quantity. We take the expectation of $P_{out}^{p\mathrm{E}}(D,\lambda_s)$ w.r.t. the random variable D denoting the distance of a PRx[6] to its nearest PTx; it can be shown to have a distribution function $F_D(x) = 1 - \exp\left\{-\lambda_p \pi x^2\right\}$. So, we have

$$\mathbb{E}[P_{out}^{p\mathrm{E}}(D,\lambda_s)] = \int_0^{d_p} P_{out}^{p\mathrm{E}}(d,\lambda_s)dF_D(x) + e^{-\lambda_p \pi d_p^2}. \quad (7)$$

C. Outage Probability of Outdoor Secondary Receiver

In this section, we consider the outage probability $P_{out}^{so\mathrm{E}}$ of a typical E-oSRx denoted here by W_o. This is a conditional

[6]As discussed in Section III-A, here PRx Y doe not necessarily belong to Π_r.

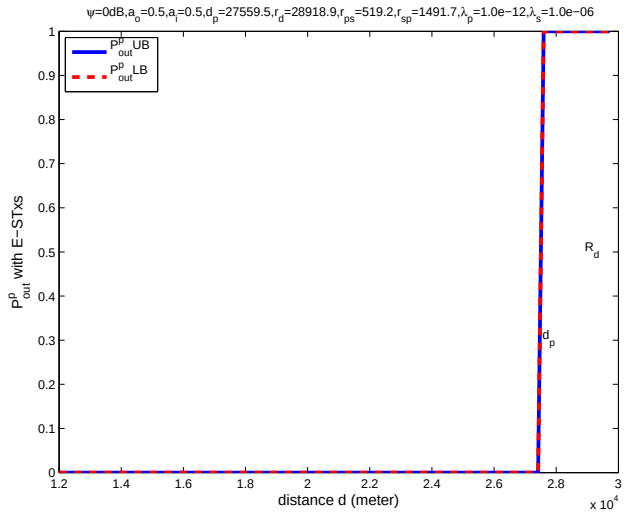

(a) If there is no indoor nodes (i.e., $\psi = 0$), setting $r_d = d_p + r_{sp}(d_p)$ is enough to protect PRxs from STxs' interference. Note that PRx's outage is zero for $d < d_p$.

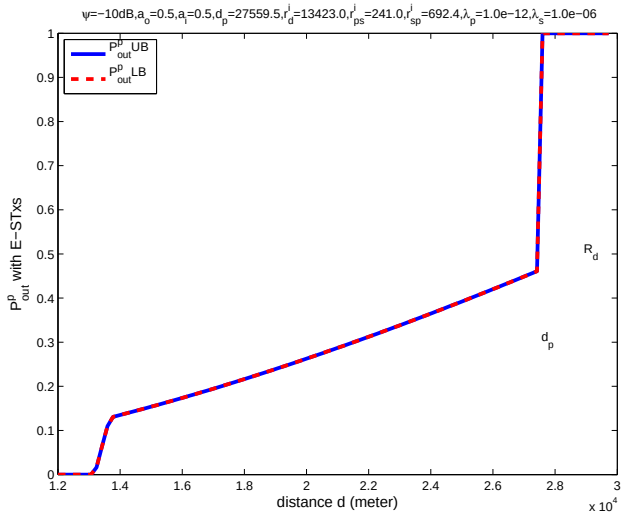

(b) If there exist 50% of indoor nodes ($a_i = 0.5$) with $\psi = -10$dB, they mis-detect the existence of nearby PTx and start transmitting even when they are inside the coverage i.e., when $d < d_p$. It causes severe increase of PRx's outage probability.

Fig. 3: Impact of STxs' interference to outage probability of PRx at distance d to its nearest PTx

outage probability conditioned on the existence of an active E-oSTx Z_o transmitting to an E-oSRx W_o as shown in Fig.9. Note that Z_o is not necessarily the nearest E-oSTx to the W_o. This can be viewed as a worst case analysis since we fix $\|W_o - Z_o\|$ to be d_s. For the E-oSTx Z_o to be active, there should be no PTxs within the E-oSTx's detection area; so, we condition on the event $Z_o \notin B\left(\Pi_p, r_d^{\mathrm{E}}\right)$ and $\|W_o - Z_o\| = d_s$. Note that interference from other E-STxs can cause an outage at the the E-oSRx W_o. In the following therefore, we capture the impact from PTxs, E-oSTxs, and E-iSTxs on the outage of a typical E-oSRx W_o.

Theorem 6. *(Conditional Outage Probability of E-oSRx): For given λ_p and λ_s, the conditional outage probability of a E-oSRx whose associated transmitter E-oSTx is a distance d_s away is given by*

$$P_{out}^{so\mathrm{E}}(\lambda_s) = 1 - \mathcal{L}_{\{a_o Q(r_{ss}^{oo}, \Pi_p^{(3)}, r_d^{\mathrm{E}}) + a_i Q(r_{ss}^{io}, \Pi_p^{(3)}, r_d^{\mathrm{E}i})\}}(\lambda_s),$$

where $\Pi_p^{(3)} = \Pi_p \cap \overline{b(Z_o, r_d^{\mathrm{E}}) \cup b(W_o, r_{ps})}$ and $Q\left(r, \Pi, t\right) \equiv \int_{b(W_o,r)} \mathbf{1}\left\{z \notin B\left(\Pi, t\right)\right\} dz$.

Proof is given in Appendix B. We can again provide upper and lower bounds on $P_{out}^{so\mathrm{E}}$ which can be computed numerically [38] as follows.

Corollary 7. *For given λ_p and λ_s, the upper and lower bounds of a E-oSRx's outage probability whose active associated E-oSTx is a distance d_s away are given as follows:*

$$P_{out}^{so\mathrm{E},u}(\lambda_s) = 1 - \exp\left\{-\lambda_s q_{\mathrm{E}}^o\right\} \quad \text{and}$$
$$P_{out}^{so\mathrm{E},l}(\lambda_s) = \frac{q_{\mathrm{E}}^o}{q_m^o}\left(1 - \exp\left\{-\lambda_s q_m^o\right\}\right),$$

where $q_{\mathrm{E}}^{oo} = \mathbb{E}_p[Q(r_{ss}^{oo}, \Pi_p^{(3)}, r_d^E)]$, $q_{\mathrm{E}}^{io} = \mathbb{E}_p[Q(r_{ss}^{io}, \Pi_p^{(3)}, r_d^{Ei})]$, $q_{\mathrm{E}}^o = a_o q_{\mathrm{E}}^{oo} + a_i q_{\mathrm{E}}^{io}$, and q_m^o is defined in Section II-F.

Similarly, it is straightforward to compute $P_{out}^{si\mathrm{E}}(\lambda_s)$ the outage probability of a typical E-iSRx. We omit it due to space limitations.

Fig.4 shows $P_{out}^{so\mathrm{E}}(\lambda_s)$ and $P_{out}^{si\mathrm{E}}(\lambda_s)$ the outage probabilities of a typical E-oSRx and E-iSRx respectively. They were evaluated under $\psi = -10$dB. As λ_s increases, both E-oSRxs and E-iSRxs are getting more interference from neighboring E-oSTxs and E-iSTxs, which accordingly increase the outage probabilities. Note that E-iSRxs get less interference, due to indoor shadowing, than E-oSRxs, so they see better (lower) outage probability.

Remark 8. We note that E-iSTx's having smaller outage probability than that of E-oSTx is phenomenon that occurs even under other white space detection techniques in Section V and VI as long as $\psi < 1$. This lessens our burden on computing outage probabilities since we only care about the worst case outage probability. In fact, the maximum contention density of STxs under an outage constraint, which is computed in Section VII, is driven by the worst case outage probability. So, in the sequel, we will focus only on the outage probability for a typical outdoor nodes.

V. Performance of Positioning-Assisted Technique

In this section, we evaluate the outage probabilities of a PRx, G-oSRx and G-iSTx. We assume a G-STx can access its exact location relative to PTxs using a geographic positioning module and determine whether to transmit or not. A G-STx can only transmit if it is outside of PTxs' coverage area. This is equivalent to G-STxs that are able to detect PTxs within a range r_d. We define following two processes Π_{so}^{G} and Π_{si}^{G}, denoting active G-oSTxs and G-iSTxs with densities $a_o\lambda_s \mathbf{1}\left\{z \notin B\left(\Pi_p, r_d\right)\right\}$ and $a_i\lambda_s \mathbf{1}\left\{z \notin B\left(\Pi_p, r_d\right)\right\}$ at $z \in \mathbf{R}^2$ respectively. The machinery used to find outage

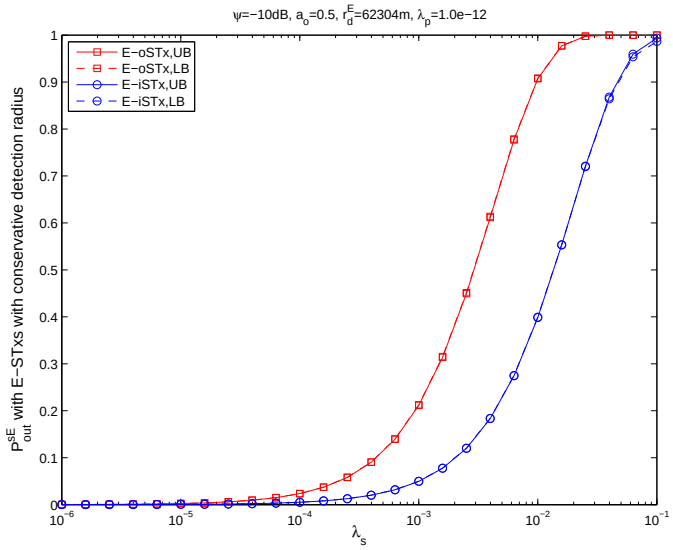

Fig. 4: The outage probability of a typical E-oSTx and E-iSTx are shown. The gap between outage probability of E-oSTx and that of E-iSTx comes from the attenuated interference from outside to E-iSTxs.

probabilities is similar to that used earlier for the densities of these two processes.

A. Outage Probability of Primary Receiver

Since G-STxs are at least a distance r_d away from PRxs, they can not give harmful interference to PRxs. Thus, we have a simple result for the outage probability of a PRx.

Fact 9. *The outage probability of PRx with G-STxs is given as* $P_{out}^{p\mathrm{G}}(d) = 1 - \mathbf{1}\{d < d_p\}$ *where* d *is the distance to its nearest PTx, and the fraction of* $\mathbf{R}^2$ *where potential PRxs can successfully receive PTxs' signal is given by* $P_c^{\mathrm{G}}(\lambda_p) = 1 - \mathbb{E}[P_{out}^{p\mathrm{G}}(D)] = 1 - \exp\{-\lambda_p \pi d_p^2\}$.

B. Outage Probability of Outdoor Secondary Receiver

In this section, we compute the outage probability $P_{out}^{so\mathrm{G}}$ of a typical G-oSRx W_o. This is a conditional outage probability conditioned on the existence of an active G-oSTx Z_o transmitting to the G-oSRx W_o. Note that Z_o is not necessarily the nearest G-oSTx to the W_o. This is the worst case outage probability since we fix $\|W_o - Z_o\|$ to d_s. For the G-oSTx Z_o to be active, there should be no PTxs within the G-oSTx's detection area; so, we condition on the event $Z_o \notin B(\Pi_p, r_d)$ and $\|W_o - Z_o\| = d_s$. Interference from other G-oSTxs and G-iSTxs to the G-oSRx W_o can cause the outage. The following theorem captures the impact of both PTxs, G-oSTxs, and G-iSTxs, on the outage of a typical G-oSRx W_o; a proof is given in the Appendix C.

Theorem 10. *(Conditional Outage Probability of G-oSRx) For a given* λ_p *and* λ_s*, the conditional outage probability of a G-oSRx at a distance* d_s *from its active associated G-oSTx is given by*

$$P_{out}^{so\mathrm{G}}(\lambda_s) = 1 - \mathcal{L}_{\{a_o Q(r_{ss}^{oo}, \Pi_p^{(4)}, r_d) + a_i Q(r_{ss}^{io}, \Pi_p^{(4)}, r_d)\}}(\lambda_s),$$

where $\Pi_p^{(4)} = \Pi_p \cap \overline{b(Z_o, r_d) \cup b(W_o, r_{ps})}$ *and* $Q(r, \Pi, t) \equiv \int_{b(W_o, r)} \mathbf{1}\{z \notin B(\Pi, t)\}\, dz$.

Corollary 11. *For given* λ_p *and* λ_s*, the upper and lower bounds of a G-oSRx's outage probability are given as follows:*

$$P_{out}^{so\mathrm{G},u}(\lambda_s) = 1 - \exp\{-\lambda_s q_{\mathrm{G}}^o\}, \quad \text{and}$$
$$P_{out}^{so\mathrm{G},l}(\lambda_s) = \frac{q_{\mathrm{G}}^o}{q_m^o}\left(1 - \exp\{-\lambda_s q_m^o\}\right)$$

where $q_{\mathrm{G}}^{oo} = \mathbb{E}_p[Q(r_{ss}^{oo}, \Pi_p^{(4)}, r_d)]$, $q_{\mathrm{G}}^{io} = \mathbb{E}_p[Q(r_{ss}^{io}, \Pi_p^{(4)}, r_d)]$ *and* $q_{\mathrm{G}}^o = a_o q_{\mathrm{G}}^{oo} + a_i q_{\mathrm{G}}^{io}$.

The value of q_{G}^{oo} and q_{G}^{io} can be computed numerically, see [38]. We omit the computation of $P_{out}^{si\mathrm{G}}$ the outage probability of a typical G-iSRx.

VI. Performance of Receiver Location-Aware Technique

In this section, we consider the outage probabilities of a PRx and L-oSRx. Since L-STxs can detect the exact location of PRxs, they are allowed to transmit even if they lie within the coverage area of PTxs as long as neighboring PRxs are not harmed. We will set the detection radius for L-oSTx to $r_d^{\mathrm{L}} = d_s + r_{ps}$, which accordingly determines the effective detection radius of L-iSTx as $r_d^{\mathrm{L}i} = \psi^{\frac{1}{\alpha}} r_d^{\mathrm{L}}$. Note that this choice will ensure that L-STx protect its L-SRxs from hidden PTxs. Note that we have $r_d^{\mathrm{L}} \ll r_d^{\mathrm{E}}$, i.e., since we can detect and protect nearby PRxs directly r_d^{L} does not need to be as large as before.

A. Outage Probability of Primary Receiver

Since L-STxs do not give any harmful interference to PRxs, the outage probability of a PRx is given as follows:

Fact 12. *The outage probability of a PRx with L-STxs is given as* $P_{out}^{p\mathrm{L}}(d) = 1 - \mathbf{1}\{d \le d_p\}$. *And the fraction of* R^2 *where potential PRxs can successfully receive STxs' signal is given as* $P_c^{\mathrm{L}}(\lambda_p) = 1 - \mathbb{E}[P_{out}^{p\mathrm{L}}(D)] = 1 - \exp\{-\lambda_p \pi d_p^2\}$.

B. Outage Probability of Secondary Receiver

In this section, we consider the outage probability of L-SRxs. As before, we focus on the outage probability of L-oSRx $P_{out}^{so\mathrm{L}}$ since it is higher than that of L-iSRxs. Note that L-oSTxs are allowed to transmit inside the coverage area of PTx, which makes $P_{out}^{so\mathrm{L}}$ for nodes inside the coverage area different than that of those which are outside. If an active L-oSRx is located within the coverage area of PTxs, then it is likely to have fewer potential interferers than an L-oSRx that is outside the coverage area. Indeed PRxs inside the coverage will suppress the activity of potential interferers L-STxs. By contrast there are no PRxs outside the coverage area, so L-oSRxs in this region are likely to see more interferers. To make this formal, we first define two subsets $\mathcal{C}_o$ and $\mathcal{N}_o$ of $\mathbf{R}$ distinguishing two regions for L-oSRxs in terms of its distance to its nearest PTx d. If $d \in \mathcal{C}_o \equiv [r_{ps} + d_s, s_o)$, the L-oSRx is inside the PTx's coverage, while if $d \in \mathcal{N}_o \equiv [s_o, \infty)$, then it is outside. We have $\mathcal{C}_o$ exclude $(0, r_{ps} + d_s)$ because if

$d \in (0, r_{ps} + d_s)$, then the L-SRx will see an outage because it is too close to the PTx, i.e., this region is not of interest. The value s_o is a conservatively selected boundary for the coverage area which is similar to d_p but smaller than d_p. [7] In the sequel, when we compute the outage probability of a L-oSRx at distance d to its nearest PTx, we will suppose that if $d \in \mathcal{N}_l$ its associated L-oSTx and its potential secondary interferers see no surrounding PRxs ($\lambda_r = 0$) that they can interfere with, while if $d \in \mathcal{C}_o$, then the L-oSTx and its potential secondary interferers will see a non-zero uniform density of PRxs ($\lambda_r > 0$) they can interfere with. Note that introducing two sets $\mathcal{N}_o$ and $\mathcal{C}_o$ is a simplification since at the vicinity of d_p, there is a region where the density of PRx is non-uniform. By treating this intermediate region as outside of coverage, we simplify our computation. Also note that this is a conservative approximation since the computed outage probability under this assumption is higher than actual outage probability. Further details on the selection of s_o are explained in [38]. Using a similar argument for L-iSTx we can decide $\mathcal{C}_i = [r^i_{ps} + d_s, s_i)$, and $\mathcal{N}_i = [s_i, \infty)$, where s_i is the unique solution of $s_i + r^{oi}_{ss} + r^i_{sp}(d_p) = d_p$. Above observation is summarized as following fact.

Fact 13. *Let $P^{so\mathrm{L}}_{out}(d)$ be the conditional outage probability of a L-oSRx at a distance d to its nearest PTx. Then, we have $P^{so\mathrm{L}}_{out}(x) \leq P^{so\mathrm{L}}_{out}(y)$ for any $x \in \mathcal{C}_o$ and $y \in \mathcal{N}_o$.*

This implies that fewer contending L-oSTxs are allowed outside of PTx's coverage area than inside. Since our focus is on the worst case, we only compute the outage probability of L-oSTxs in $\mathcal{N}_o$.

Before computing the outage probability, we let Π^{L}_{so} and Π^{L}_{si} denote Cox processes modeling L-oSTxs and L-iSTxs with densities $a_o \mathbf{1}\{T_o(z, \Pi_r)\}\mathbf{1}\left\{z \notin B(\Pi_p, r^{\mathrm{L}}_d)\right\}$ and $a_i \mathbf{1}\{T_i(z, \Pi_r)\}\mathbf{1}\left\{z \notin B(\Pi_p, r^{\mathrm{L}i}_d)\right\}$ at $z \in \mathbf{R}^2$ respectively, where $T_o(z, \Pi_r)$ is an event defined as

$$T_o(z, \Pi_r) \equiv \left\{ \begin{array}{c} \text{L-oSTx at } z \text{ does not detect PRxs in } \Pi_r \\ \text{that it could potentially interfere with} \end{array} \right\}.$$

Note that $\mathbf{1}\{T_o(z, \Pi_r)\}$ is a random variable which is a function of $z \in \mathbf{R}^2$ and Π_r. If the distance between z and its nearest PTx belongs to $\mathcal{N}_o$, we have $\mathbf{1}\{T_o(z, \Pi_r)\} = 1$ with probability 1. Also the event $T_i(z, \Pi_r)$ can be defined in similar way and we have $\mathbf{1}\{T_i(z, \Pi_r)\} = 1$ for z whose distance to its nearest PTx belongs to $\mathcal{N}_i$. Then, the outage probability of a L-oSRx distance $d \in \mathcal{N}_o$ away from its nearest PTx is given in the following theorem, which is proven in the Appendix D.

Theorem 14. *(Conditional Outage Probability of L-oSRx) For given λ_p and λ_s, the outage probability of a L-oSRx a distance $d \in \mathcal{N}_o$ away from its nearest PTx is given as follows:*

$$P^{so\mathrm{L}}_{out}(d, \lambda_s) = 1 - \mathcal{L}_{\{a_o Q(r^{oo}_{ss}, \Pi^{(5)}_p, r^{\mathrm{L}}_d) + a_i Q(r^{io}_{ss}, \Pi^{(5)}_p, r^{\mathrm{L}i}_d)\}}(\lambda_s)$$

where $\Pi^{(5)}_p = \Pi_p \cap \overline{b(Z_o, r^{\mathrm{L}}_d) \cup b(W_o, s_o)}$, and $Q(r, \Pi, t) \equiv \int_{b(W_o, r)} \mathbf{1}\{z \notin B(\Pi, t)\}\, dz$.

[7] Specifically, s_o is the unique solution of $s_o + r^{oo}_{ss} + r_{sp}(d_p) = d_p$, see [38] for further detail.

We provide the upper and lower bounds of $P^{soL}_{out}(d)$.

Corollary 15. *For given λ_p and λ_s, upper and lower bounds on the outage probability of a L-oSRx a distance $d \in \mathcal{N}_o$ away from its nearest PTx are given as*

$$P^{so\mathrm{L},u}_{out}(d, \lambda_s) = 1 - \exp\{-\lambda_s q^o_{\mathrm{L}}\} \quad \textit{and} \tag{8}$$

$$P^{so\mathrm{L},l}_{out}(d, \lambda_s) = \frac{q^o_{\mathrm{L}}}{q^o_m}\left(1 - \exp\{-\lambda_s q^o_m\}\right), \tag{9}$$

where $q^o_{\mathrm{L}} = a_o q^{oo}_{\mathrm{L}} + a_i q^{io}_{\mathrm{L}}$, $q^{oo}_{\mathrm{L}} = \mathbb{E}[Q(r^{oo}_{ss}, \Pi^{(5)}_p, r^{\mathrm{L}}_d)]$ and $q^{io}_{\mathrm{L}} = \mathbb{E}[Q(r^{io}_{ss}, \Pi^{(5)}_p, r^{\mathrm{L}i}_d)]$.

q^{oo}_{L} and q^{io}_{L} can be computed numerically, see [38].

Fact 16. *Note that for $d \in \mathcal{N}_o$, we have $q^{oo}_{\mathrm{L}} = q^{oo}_m$, and $q^{io}_{\mathrm{L}} = q^{io}_m$, since q^{oo}_m and q^{io}_m are constants, consequently the upper and lower bounds of $P^{so\mathrm{L}}_{out}$ are not affected by d as $P^{so\mathrm{E}}_{out}$ and $P^{so\mathrm{G}}_{out}$ aren't.*

Using a similar approach, we can also compute the outage probability of L-iSRx $P^{si\mathrm{L}}_{out}(d)$.

VII. Maximum Contention Density for Secondary Nodes given ϵ-outage constraint

In this section, we will find the maximum contention densities of STxs for each white space detection technique under an ϵ-outage constraint where $0 < \epsilon < 1$ and $\overline{\epsilon} = 1 - \epsilon$. This density maximizes the number of concurrent active STxs while keeping the outage probability of SRxs below ϵ for a given λ_p and a_o. In the process, we will take the minimum of the outdoor and indoor contention densities, because we need to satisfy the outage constraint for both indoor and outdoor nodes.

A. Density for E-STx

Given outage probabilities $P^{so\mathrm{E}}_{out}(\lambda_s)$ and $P^{si\mathrm{E}}_{out}(\lambda_s)$ obtained for E-oSRx and E-iSRx respectively, the maximum contention density for E-SRxs which guarantees $P^{so\mathrm{E}}_{out}(\lambda_s) \leq \epsilon$ and $P^{si\mathrm{E}}_{out}(\lambda_s) \leq \epsilon$ is defined as $\lambda^{\epsilon\mathrm{E}}_s \equiv \min\left\{\lambda^{\epsilon\mathrm{E}}_{so}, \lambda^{\epsilon\mathrm{E}}_{si}\right\}$, where we have $\lambda^{\epsilon\mathrm{E}}_{so} \equiv \max\left\{\lambda_s | P^{so\mathrm{E}}_{out}(\lambda_s) \leq \epsilon\right\}$ and $\lambda^{\epsilon\mathrm{E}}_{si} \equiv \max\left\{\lambda_s | P^{si\mathrm{E}}_{out}(\lambda_s) \leq \epsilon\right\}$. We note that since interference is attenuated indoor, we can show $\lambda^{\epsilon\mathrm{E}}_{so} \leq \lambda^{\epsilon\mathrm{E}}_{si}$, and accordingly we have $\lambda^{\epsilon\mathrm{E}}_s = \lambda^{\epsilon\mathrm{E}}_{so}$. Upper and lower bounds on $\lambda^{\epsilon\mathrm{E}}_{so}$ are given as follows:

$$\lambda^{\epsilon\mathrm{E},u}_{so} \equiv \max\left\{\lambda_s | P^{so\mathrm{E},l}_{out}(\lambda_s) \leq \epsilon\right\} = -\frac{1}{q^o_m}\log\left(1 - \frac{q^o_m}{q^o_{\mathrm{E}}}\epsilon\right),$$

$$\lambda^{\epsilon\mathrm{E},l}_{so} \equiv \max\left\{\lambda_s | P^{so\mathrm{E},u}_{out}(\lambda_s) \leq \epsilon\right\} = -\frac{\log\overline{\epsilon}}{q^o_{\mathrm{E}}}.$$

Note that $\lambda^{\epsilon\mathrm{E}}_s$ is a function of λ_p.

B. Density for G-STx

For the given outage probabilities $P^{so\mathrm{G}}_{out}(\lambda_s)$ and $P^{si\mathrm{G}}_{out}(\lambda_s)$ obtained for G-oSRx and G-iSRx respectively, the maximum contention density for G-STxs which guarantees $P^{so\mathrm{G}}_{out}(\lambda_s) \leq \epsilon$ and $P^{si\mathrm{G}}_{out}(\lambda_s) \leq \epsilon$ is given by $\lambda^{\epsilon\mathrm{G}}_s \equiv \min\left\{\lambda^{\epsilon\mathrm{G}}_{so}, \lambda^{\epsilon\mathrm{G}}_{si}\right\}$ where $\lambda^{\epsilon\mathrm{G}}_{so} \equiv \max\left\{\lambda_s | P^{so\mathrm{G}}_{out}(\lambda_s) \leq \epsilon\right\}$ and

$\lambda_{si}^{\epsilon \mathrm{G}} \equiv \max\left\{\lambda_s | P_{out}^{si\mathrm{G}}(\lambda_s) \leq \epsilon\right\}$. Analogously with the previous case, we can show that $\lambda_{so}^{\epsilon \mathrm{G}} \leq \lambda_{si}^{\epsilon \mathrm{G}}$, and accordingly we have $\lambda_s^{\epsilon \mathrm{G}} = \lambda_{so}^{\epsilon \mathrm{G}}$. Upper and lower bounds of $\lambda_{so}^{\epsilon \mathrm{G}}$ are given by

$$\lambda_{so}^{\epsilon \mathrm{G},u} \equiv \max\left\{\lambda_s | P_{out}^{so\mathrm{G},l}(\lambda_s) \leq \epsilon\right\} = -\frac{1}{q_m^o}\log\left(1 - \frac{q_m^o}{q_{\mathrm{G}}^o}\epsilon\right),$$

$$\lambda_{so}^{\epsilon \mathrm{G},l} \equiv \max\left\{\lambda_s | P_{out}^{so\mathrm{G},u}(\lambda_s) \leq \epsilon\right\} = -\frac{\log\overline{\epsilon}}{q_{\mathrm{G}}^o}.$$

Note that $\lambda_s^{\epsilon \mathrm{G}}$ is a function of λ_p.

C. Density for L-STx

Note that in Section VI, we found the outage probability for a L-oSRx as a function of its distance d from its closest PTx, so the corresponding contention density will be also a function of d. For the outage probabilities $P_{out}^{so\mathrm{L}}(\lambda_s)$ and $P_{out}^{si\mathrm{L}}(\lambda_s)$ obtained for L-oSRx and L-iSRx respectively, the maximum contention density $\lambda_s^{\epsilon \mathrm{L}}$ is defined as $\lambda_s^{\epsilon \mathrm{L}} \equiv \min\left\{\min_{d\in\mathcal{C}_o\cup\mathcal{N}_o}\lambda_{so}^{\epsilon \mathrm{L}}(d), \min_{d\in\mathcal{C}_i\cup\mathcal{N}_i}\lambda_{si}^{\epsilon \mathrm{L}}(d)\right\}$, where $\lambda_{so}^{\epsilon \mathrm{L}}(d) \equiv \max\left\{\lambda_s | P_{out}^{so\mathrm{L}}(d,\lambda_s) \leq \epsilon\right\}$ and $\lambda_{si}^{\epsilon \mathrm{L}}(d) \equiv \max\left\{\lambda_s | P_{out}^{si\mathrm{L}}(d,\lambda_s) \leq \epsilon\right\}$. Fact 13 implies that $\lambda_{so}^{\epsilon \mathrm{L}}(x) \geq \lambda_{so}^{\epsilon \mathrm{L}}(y)$ for $x \in \mathcal{C}_o$ and $y \in \mathcal{N}_o$, and $\lambda_{si}^{\epsilon \mathrm{L}}(x) \geq \lambda_{si}^{\epsilon \mathrm{L}}(y)$ for $x \in \mathcal{C}_i$ and $y \in \mathcal{N}_i$. It follows once again that $\lambda_{so}^{\epsilon \mathrm{L}}(d) \leq \lambda_{si}^{\epsilon L}(d)$. By Fact 16, it turns out that $\lambda_s^{\epsilon \mathrm{L}} = \lambda_{so}^{\epsilon \mathrm{L}}$ is not a function of d. Upper and lower bounds of $\lambda_{so}^{\epsilon L}$ are defined as

$$\lambda_{so}^{\epsilon \mathrm{L},u} \equiv \max\left\{\lambda_s | P_{out}^{so\mathrm{L},l}(\lambda_s) \leq \epsilon\right\} = -\frac{1}{q_m^o}\log\left(1 - \frac{q_m^o}{q_{\mathrm{L}}^o}\epsilon\right),$$

$$\lambda_{so}^{\epsilon \mathrm{L},l} \equiv \max\left\{\lambda_s | P_{out}^{so\mathrm{L},u}(\lambda_s) \leq \epsilon\right\} = -\frac{\log\overline{\epsilon}}{q_{\mathrm{L}}^o}.$$

Note that $\lambda_s^{\epsilon \mathrm{L}}$ is a function of λ_p.

VIII. Joint Network Capacity Region

In this section, we define and compute the capacity of primary and secondary networks using the outage probability and contention densities computed in the previous sections. This will enable us to compute the joint network capacity region exhibiting trade-offs between the two networks.

A. Broadcast Coverage Capacity of Primary Network

The capacity of the primary network coexisting with E-STxs is defined as the mean number of bits that can be successfully received by potential PRxs per second per meter square per Hertz. It is given as b_p times the fraction of effectively covered area by PTxs in (7) as follows:

$$C_1^{\mathrm{E}}(\lambda_p, \psi) = b_p P_c^{\mathrm{E}}\left(\lambda_p, \lambda_s^{\epsilon \mathrm{E}}, \psi\right).$$

Similarly, the capacity of primary network with G-STxs and L-STxs can be computed using P_c^{G} and P_c^{L}, they are denoted C_1^{G} and C_1^{L} respectively.

B. Transmission Capacity of Secondary Network

The notion of capacity for secondary network, which we adopt from [12], [27], is the transmission capacity measuring the average number of successfully transmitted bits per square meter per Hertz.

Transmission Capacity of Secondary Network with E-STxs: For given λ_p and a_o, the capacity of a secondary network with E-STxs is defined as the sum of outdoor and indoor transmission capacities C_2^{Eo} and C_2^{Ei}:

$$\begin{aligned} C_2^{\mathrm{E}}(\lambda_p, \psi, a_o) &= C_2^{\mathrm{Eo}} + C_2^{\mathrm{Ei}} \\ &= b_s a_o \lambda_s^{\epsilon \mathrm{E}} P_{tx}^{\mathrm{E}o}\overline{\epsilon} + b_s a_i \lambda_s^{\epsilon \mathrm{E}} P_{tx}^{\mathrm{E}i}\overline{\epsilon}, \end{aligned}$$

where $P_{tx}^{\mathrm{E}o} = \exp\{-\lambda_p \pi (r_d^E)^2\}$ and $P_{tx}^{\mathrm{E}i} = \exp\{-\lambda_p \pi (r_d^{Ei})^2\}$ are the transmission probabilities of a typical E-oSTx and E-iSTx respectively. Recall that for an E-oSTx (E-iSTx) to transmit it should detect the absence of PTxs in its corresponding detection region. A larger detection radius is good to protect PRxs and its intended SRx but reduces exponentially its transmission opportunity. Note that $\lambda_s^{\epsilon \mathrm{E}}$ is also a function of λ_p.

Transmission Capacity of Secondary Network with G-STxs: For a given λ_p and a_o, the capacity of a secondary network with G-STxs is defined as the sum of outdoor and indoor transmission capacities $C_2^{\mathrm{G}o}$ and $C_2^{\mathrm{G}i}$ respectively:

$$\begin{aligned} C_2^{\mathrm{G}}(\lambda_p, \psi, a_o) &= C_2^{\mathrm{G}o} + C_2^{\mathrm{G}i} \\ &= b_s a_o \lambda_s^{\epsilon \mathrm{G}} P_{tx}^{\mathrm{G}o}\overline{\epsilon} + b_s a_i \lambda_s^{\epsilon \mathrm{G}} P_{tx}^{\mathrm{G}i}\overline{\epsilon}, \end{aligned}$$

where $P_{tx}^{\mathrm{G}o} = \exp\left\{-\lambda_p \pi r_d^2\right\}$ and $P_{tx}^{\mathrm{G}i} = \exp\left\{-\lambda_p \pi r_d^2\right\}$ are the transmission probabilities of G-oSTx and G-iSTx respectively. Note that $\lambda_s^{\epsilon \mathrm{G}}$ is a function of λ_p.

Transmission Capacity of Secondary Network with L-STxs: For a given λ_p, λ_r, and a_o, the capacity of a secondary network with L-STxs is defined as the expected value of the sum of two transmission capacities:

$$C_2^{\mathrm{L}}(\lambda_p, \lambda_r, \psi, a_o) = C_2^{\mathrm{L}} = \mathbb{E}\left[C_2^{\mathrm{L}o}(D) + C_2^{\mathrm{L}i}(D)\right],$$

where $C_2^{\mathrm{L}o}(D) \equiv b_s a_o \lambda_s^{\epsilon \mathrm{L}} P_{tx}^{\mathrm{L}o}(D)\,\overline{\epsilon}$ and $C_2^{\mathrm{L}i}(D) \equiv b_s a_i \lambda_s^{\epsilon \mathrm{L}} P_{tx}^{\mathrm{L}i}(D)\,\overline{\epsilon}$ are the conditional capacities of a L-oSRx and a L-iSRx when they are located at distance D from its nearest PTx. Note that $\lambda_s^{\epsilon \mathrm{L}}$ is not a function of D. The expected value can be computed as follows:

$$\begin{aligned} &\mathbb{E}\left[C_2^{\mathrm{L}o}(D)\right] \\ &= \sum_{\mathcal{A}\in\{\mathcal{C}_0,\mathcal{N}_0\}} \mathbb{E}\left[C_2^{\mathrm{L}o}(D)\,|D\in\mathcal{A}\right] P(D\in\mathcal{A}) \\ &= b_s a_o \lambda_s^{\epsilon \mathrm{L}}\overline{\epsilon} \sum_{\mathcal{A}\in\{\mathcal{C}_0,\mathcal{N}_0\}} \mathbb{E}\left[P_{tx}^{\mathrm{L}o}(D)\,|D\in\mathcal{A}\right] P(D\in\mathcal{A}) \\ &= b_s a_o \lambda_s^{\epsilon \mathrm{L}}\overline{\epsilon}\left(P_{tx}^{\mathrm{L}oc} P(D\in\mathcal{C}_o) + P_{tx}^{\mathrm{L}on} P(D\in\mathcal{N}_o)\right), \end{aligned}$$

Similarly, we have

$$\mathbb{E}[C_2^{\mathrm{L}i}(D)] = b_s a_i \lambda_s^{\epsilon \mathrm{L}}\overline{\epsilon}(P_{tx}^{\mathrm{L}ic} P(D\in\mathcal{C}_i) + P_{tx}^{\mathrm{L}in} P(D\in\mathcal{N}_i)),$$

where, $P_{tx}^{\mathrm{L}oc}$, $P_{tx}^{\mathrm{L}on}$, $P_{tx}^{\mathrm{L}ic}$ and $P_{tx}^{\mathrm{L}in}$ are conditional transmission probabilities of L-oSTx when $d\in\mathcal{C}_o$ and $d\in\mathcal{N}_o$ and that of L-iSTx when $d\in\mathcal{C}_i$ and $d\in\mathcal{N}_i$ respectively. They are computed as $P_{tx}^{\mathrm{L}oc} = \mathbb{E}[\exp\{-\lambda_r \pi r_{sp}^2(D)\}|D\in\mathcal{C}_o]$, and $P_{tx}^{\mathrm{L}ic} = \mathbb{E}[\exp\{-\lambda_r \pi (r_{sp}^i(D))^2\}|D\in\mathcal{C}_i]$ and $P_{tx}^{\mathrm{L}on} = P_{tx}^{\mathrm{L}in} = 1$. These can be numerically computed since distribution of D is known. And, it is straightforward to find $P(D\in\mathcal{C}_o)$, $P(D\in\mathcal{N}_o)$, $P(D\in\mathcal{C}_i)$ and $P(D\in\mathcal{N}_i)$.

C. Joint Network Capacity Region

We define the joint network capacity region when secondary nodes using simple signal energy detection method as the set of achievable capacities for the primary and secondary networks, which is given as

$$\Lambda^{\mathrm{E}}(\psi, a_o) \equiv \{(x,y) \in \mathbf{R}^2 | \exists \lambda_p \geq 0, \text{ s.t. } x = C_1^{\mathrm{E}}(\lambda_p, \psi, a_o), 0 \leq y \leq C_2^{\mathrm{E}}(\lambda_p, \psi, a_o)\}.$$

The joint network capacity regions for positioning-assisted and receiver location-aware techniques are denoted as $\Lambda^{\mathrm{G}}(\psi, a_o)$ and $\Lambda^{\mathrm{L}}(\lambda_r, \psi, a_o)$ respectively, that are similarly defined. Note that we have lower and upper bounds on the contention density rather than an exact value, so we get the lower (inner) and upper (outer) bounds on the capacity and joint network capacity region by replacing $\lambda_s^{\epsilon \mathrm{E}}$ with $\lambda_s^{\epsilon \mathrm{E},u}$ or $\lambda_s^{\epsilon \mathrm{E},l}$. This also applies to other cases. In Figs.7-9, we only draw the lower bounds of joint network capacity regions since upper bounds are almost on top of associated lower bounds. In all cases $\epsilon = 0.1$ was used.

Impact of indoor shadowing (signal energy detection technique): Let us consider the impact of indoor shadowing on the joint network capacity region of two networks under the signal energy detection method. Fig.5a shows the joint network capacity regions under various values of indoor shadowing ψ. We make following interesting observations. If the primary network is sparse, in the regime with relatively low C_1, as the shadowing level increases (i.e., ψ decreases), the capacity C_2 increases, further increases of ψ eventually decrease C_2, that is $C_2(\lambda_p, \psi)$ has its maximum value at some ψ^* which is the function of C_1. While if the primary network is dense, there is not much change in capacity. This can be explained in following ways. As the level of indoor shadowing increases, the E-oSRxs receive less interference from E-STxs, which decreases the outage probability of E-oSRx and eventually leads to an higher contention density. It contributes to capacity as a *gain*. But simultaneously we also have a *loss*, which comes from the decreasing transmission probability caused by over-conservatively increasing detection radius. It discourages the transmission attempts of E-oSTxs and have a negative impact on capacity. The capacity increases if the increase of contention density dominates the decrease of transmission probability. And, the capacity decreases otherwise. Consider increasing shadowing level, then, the point that the loss dominates the gain comes late as the primary network gets sparse since the more sparse the primary network is, the more E-oSTxs it can accommodate. So, capacity C_2 in sparse network has its maximum at a certain ψ value. While, in dense network, both the gain and loss are comparable and are balanced so there is not much change in capacity.

Impact of indoor shadowing (positioning-assisted technique): We consider the impact of indoor shadowing on the joint network capacity region under positioning method, see Fig.5b. In this case, the joint network capacity region strictly increases as shadowing level increases. This is explained as follows. Recall that the detection performance of the positioning assisted method is not affected by indoor shadowing, so they can correctly detect the existence of PTxs within their detection radius r_d. Thus, there is no loss in transmission probability. However, the level of interference from other nodes is affected by the indoor shadowing level ψ. It turns out that there is only *gain* without *loss* as compared to signal energy detection case. In fact, as the shadowing level increases, G-oSRxs get less interference from G-iSRxs due to strong attenuation, which eventually allows a higher maximum contention density. Thus, we have only *gain*, which results in a strict increase of C_2 with ψ for all C_1. The actual *gain of indoor shadowing* depends on the level of indoor shadowing,

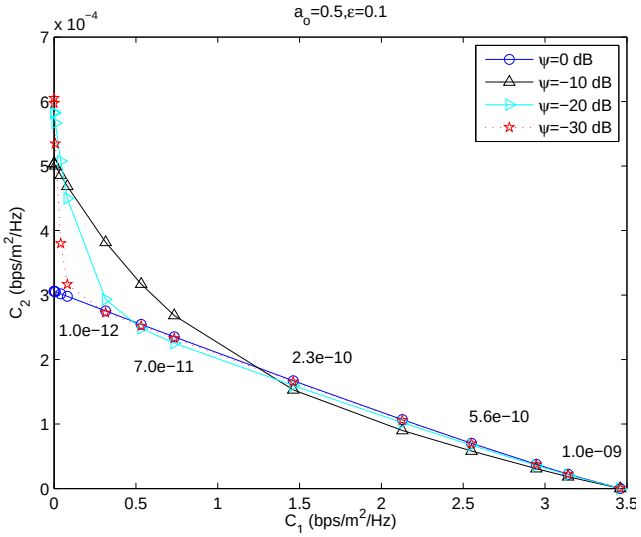

(a) joint network capacity regions under the signal energy detection method were shown for various values of indoor shadowing level ψ. If $\psi = 0$dB, then the we have roughly linear tradeoff. As the shadowing level increases (as ψ decreases), network capacity region increases but after a certain point, it decreases.

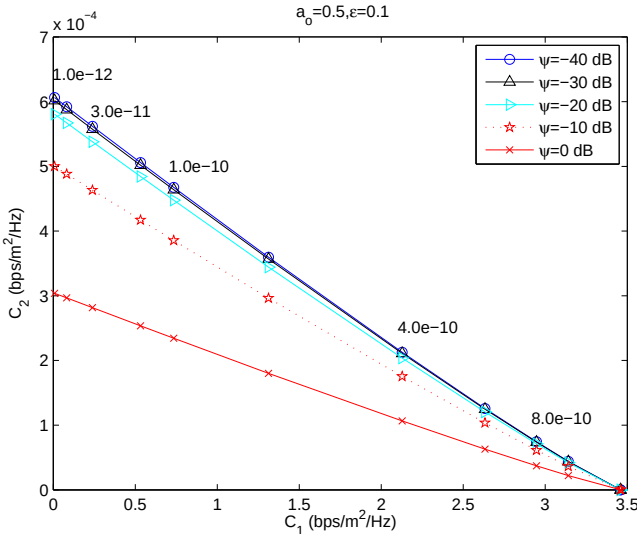

(b) Joint network capacity regions under the positioning-assisted method were shown for various values of indoor shadowing level ψ. The network capacity region increases strictly in ψ for all C_1 as the shadowing level increases.

Fig. 5: Joint network capacity regions of signal energy detection method (left) and positioning-assisted method (right) under various indoor shadowing level ψ with fixed $a_o = 0.5$. The numbers above/below markers in graphs denote the density of PTxs λ_p at the collection of markers with the similar C_1 values.

e.g. when $\psi = -10$dB, the gain (compared to $\psi = 0$dB case) is approximately 66% and when $\psi = -20$dB, the gain is roughly 200%. If $\psi \to -\infty$dB, then, the G-SRxs are free from interference from G-iSRxs and the their performance is constrained by their self interference from G-oSTxs to G-oSRxs.

Impact of indoor shadowing (receiver location-aware technique): Fig.6a shows the joint network capacity region of the receiver location-aware method under $\lambda_r = 10^{-4}m^{-2}$. Due to the receiver detection function, more L-STxs can be active (even inside the coverage). This significantly increases the joint network capacity region. The same argument on decreased interference and resulting increased maximum density applies here. One interesting observation is that there exists a regime where both primary and secondary capacity increases together. This happens when the density of PTxs is very high. In this case L-STxs are more likely to succeed in their transmissions, since L-STxs close to PTxs require smaller region to be PRx free. Recall that those PRxs close to PTxs are receiving strong signals from PTxs, so it is hard for L-STxs to harm them. This allows a larger number of L-STxs be active close to PTxs than at the edge of the PTxs' coverage area. Fig.2c depicts this situation.

Note, however, that a further increase in λ_p forces C_2 to 0. This happens because once λ_p is large enough the entire $\mathbf{R}^2$ plane is covered by $B(\Pi_p, d_p)$ and C_1 reaches its limit 3.5. Further increases in λ_p increase the region $B(\Pi_p, r_d^{\mathrm{L}i}) = \cup_{X\in\Pi_p} b(X, r_d^{\mathrm{L}i})$ where no L-STxs are allowed to transmit. Note that $r_d^{\mathrm{L}i} \ll d_p$ and STxs can potentially interfere with PRxs if they are located inside $B(\Pi_p, r_d^{\mathrm{L}i})$. This reduces white space available to L-STxs, and accordingly C_2 eventually reaches 0. The *gain of shadowing* depends on the level of indoor shadowing, e.g. when $\psi = -10$dB gain (compared to $\psi = 0$dB case) is approximately 66% and when $\psi = -20$dB, the gain is roughly 200%. As $\psi \to -\infty$dB, interference from indoor devices to outdoor devices decreases, and the secondary capacity is limited by the self interference of L-oSTxs. The joint network capacity region is also affected by the density of primary receiver λ_r as shown in Fig.6b . If $\lambda_r = 0$, then, the activity of L-STxs are hardly affected except the extreme case when $C_1 \sim 3.5$. As λ_r increases, L-STxs lose their transmission opportunities and accordingly secondary capacity decreases. If λ_r is very high, e.g, more than 10^{-2}, then, almost no L-STxs are allowed to transmit inside PTxs' coverage area. The joint network capacity region of this case is equivalent to that of the positioning-assisted technique. Thus, the capacity trade-off is almost linear.

Impact of the Fraction of Indoor Nodes: The fraction of indoor nodes $a_i = 1 - a_o$ has a direct impact on capacity. Let us consider how the joint network capacity region changes as a function of a_o. Fig.7a-7b show the joint network capacity region for two extreme situations, where $a_o = 1$ and $a_o = 0$ respectively. The case where $a_o = 0.5$ was shown in Fig.1. The indoor shadowing level ψ is fixed to -10dB. The shapes of network capacity regions for $a_o = 1$ and $a_o = 0.5$ are similar to each other but the network capacity region for $a_o = 0$ is larger than that for $a_o = 1$. In Fig.7a, we have E-oSTxs using a very conservative detection radius, which

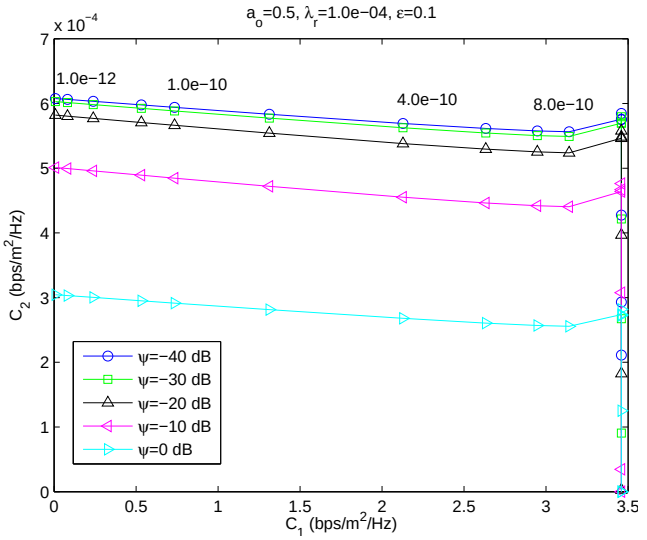

(a) Joint network capacity regions under the receiver location-aware method were shown for various values of indoor shadowing level ψ and $\lambda_r = 10^{-4}$. Increasing indoor shadowing increases the joint network capacity region. For fixed ψ, the shape of joint network capacity region depends on the density of PRxs (see right figure).

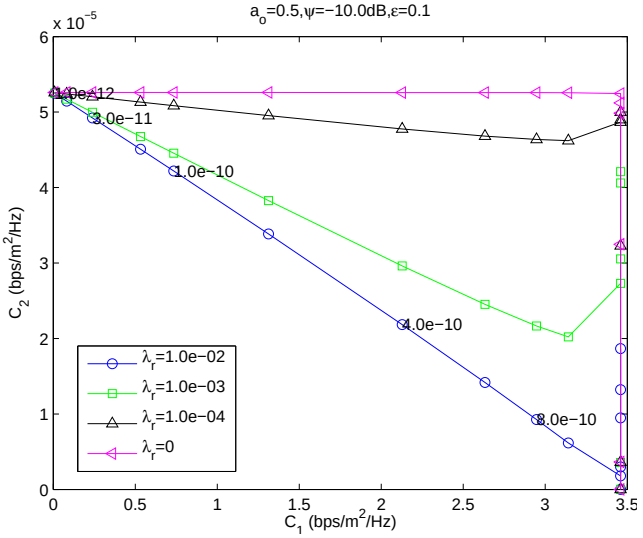

(b) The joint network capacity regions of receiver location-aware technique were shown for various values of primary receiver density λ_r. The joint network capacity region is maximized when $\lambda_r = 0$ and shrinks as λ_r increases.

Fig. 6: Joint network capacity regions under receiver location-aware technique. The numbers above markers in graphs denotes the density of PTxs λ_p at the collection of markers with the similar C_1 values.

makes them inefficiently utilize white space[8]. As the portion of indoor nodes a_i increases (or a_o decreases), iSTxs make less interference and oSTxs' outage probability decreases, which eventually allows a higher maximum contention density. C_2 increases and accordingly joint network capacity region is extended. At the other extreme with no outdoor nodes ($a_o = 0$), we have the same joint network capacity region

[8]Note that if an operator knows that there is no L-iSTxs at all, then they don't need to use conservative detection radii. Case $a_o = 1$ should be understood as the case where we have extremely small number of E-iSTxs while most are E-oSTxs. Their detection radii are set conservatively considering the E-iSTxs.

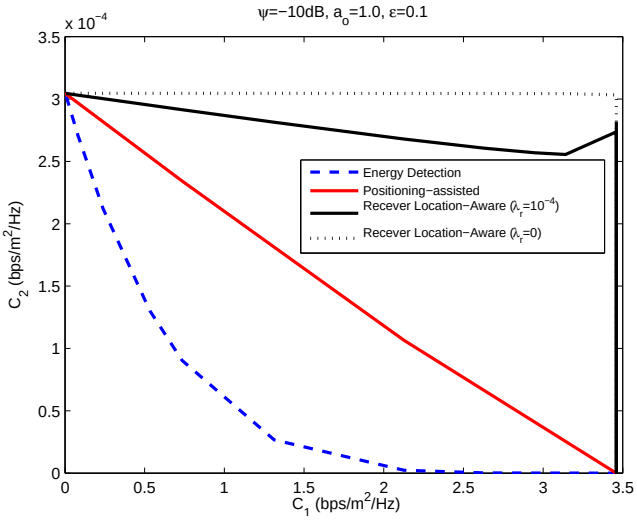

(a) Joint network capacity region when all cognitive devices are outdoor devices ($a_o = 1$). The joint network capacity regions are smaller than $a_o = 0.5$ case in Fig.1.

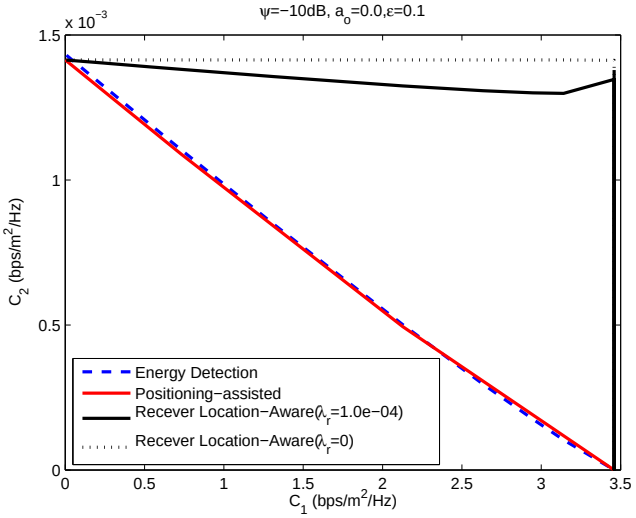

(b) Joint network capacity region when all cognitive devices are indoor devices ($a_o = 0$). The joint network capacity regions are larger than $a_o = 0.5$ case in Fig.1.

Fig. 7: Joint network capacity region under various a_o with $\psi = -10$dB. Case $a_o = 0.5$ is shown in Fig.1.

for signal energy detection technique and positioning-assisted technique since there no longer are E-oSTxs which use white spectrum inefficiently. Note that the overall network capacity region is again significantly increased as compared to the case where $a_o = 1$. When $a_o = 0.5$, as shown in Fig.1, the gain of positioning-assisted technique to signal energy detection technique is 76% and that of receiver location-aware technique is 177% when $\lambda_p = 2 \times 10^{-10} m^{-2}$. This gain can be increased further in denser primary networks. From the above two observations, we conclude that indoor shadowing, which is a source of uncertainty from signal energy detection point of view, can increase the capacity of cognitive networks. If cognitive devices can access some knowledge on their environment or additional information they can best utilize the shadowing to improve network capacity.

IX. Conclusion

In this paper, we have *quantified* the gain of three different white space detection techniques with varying degrees of RF-environment awareness under an indoor shadowing environment. Using a simple stochastic geometric model where primary and secondary nodes were modeled as Poisson point processes, we derived the joint network capacity region of two networks. It turned out that when ad hoc cognitive networks used the signal energy detection method, indoor shadowing was a source of uncertainty that could either increase or decrease the capacity of networks. However, if secondary devices had a little bit of knowledge of the environment (shadowing), then, the shadowing became the source of "hidden" capacity, i.e., they were able to achieve a significantly higher capacity in a shadowing environment. We noted that the receiver location-aware white space detection technique was by far the most promising way of detecting and filling spatial white space, while positioning-assisted technique, which still results in a large improvement over signal energy detection scheme, was inferior than receiver location-aware technique. Our results showed that enabling cognitive devices to be aware of the locations of the PRxs will lead to significant performance gains depending on the density of PRx's. We further note that this framework can be extended to evaluate advanced cognitive radio techniques requiring even more knowledge such as primary users' messages as shown in [39], [40].

References

[1] FCC, "Spectrum policy task force," *Rep. ET Docket no. 02-135*, Nov. 2002.
[2] J Mitola, III and G Maguire, Jr., "Cognitive radio: making software radios more personal," *IEEE Personal Communication*, vol. 6, pp. 13–18, Aug 1999.
[3] I. F. Akyildiz, W. Lee, M. C. Vuran, and S. Mohanty, "Next generation/dynamic spectrum access/cognitive radio wireless networks: A survey," *Elsevier Computer Network*, vol. 50, pp. 2127–2159, Sep 2006.
[4] Q. Zhao and B. M. Sadler, "A survey of dynamic spectrum access," *IEEE Signal Processing Magazine*, vol. 24, no. 3, pp. 79–89, May 2007.
[5] M. Vu, N. Devroye, and V. Tarokh, "On the primary exclusive region of cognitive networks," *IEEE Trans. Wireless Comm.*, vol. 8, pp. 3380–3385, Jul 2009.
[6] P. Gupta and P.R. Kumar, "Capacity of wireless networks," *IEEE Trans. Infomation Theory*, vol. 46, pp. 388–404, Mar 2000.
[7] B. Han and G. Simon, "Capacity of wireless ad hoc networks, a survey," *Technical Report, available at http://public.enst-bretagne.fr/∼bhan/publications/capacity-survey.pdf*, 2007.
[8] S. Jeon, N. Devroye, M. Vu, S. Chung, and V. Tarokh, "Cognitive networks achieve throughput scaling of a homogeneous network," *submitted to IEEE Trans. Infomation Theory*, 2008.
[9] C. Yin, L. Gao, and S. Cui, "Scaling laws of overlaid wireless networks: A cognitive radio network vs. a primary network," *submitted to IEEE/ACM Trans. Networking.*, 2008.
[10] K. Huang, V. K. N. Lau, and Y. Chen, "Spectrum sharing between cellular and mobile ad hoc networks: Transmission-capacity trade-off," *IEEE Jour. Select. Areas in Comm.*, 2009.
[11] C. Yin, L. Gao, T. Liu, and S. Cui, "Transmission capacities for overlaid wireless ad hoc networks with outage constraints," *IEEE Inter. Conf. on Communication (ICC)*, Jun 2009.
[12] S. P. Weber, X. Yang, J. G. Andrews, and G. de Veciana, "Transmission capacity of wireless ad hoc networks with outage constraints," *IEEE Trans. Infomation Theory*, vol. 51, pp. 4091–4102, Dec 2005.
[13] W. Ren, Q. Zhao, and A. Swami, "Power control in cognitive radio networks: How to cross a multi-lane highway," *IEEE Jour. Select. Areas in Comm.*, vol. 27, no. 7, pp. 1283–1296, Sep 2009.
[14] N. Hoven and A. Sahai, "Power scaling for cognitive radio," *WirelessCom Symposium on Emerging Networks*, vol. 1, pp. 250–255, Jun 2005.

[15] FCC, "Fcc adopts rules for unlicensed use of television white spaces.," Nov 2008, Available at http://hraunfoss.fcc.gov/edocs_public/attachmatch/FCC-08-260A1.pdf.

[16] M. A. McHenry, K. Steadman, and M. Lofquist, "Determination of detection thresholds to allow safe operation of television band "white space" devices," *Proc. IEEE DySpan*, pp. 1–12, Oct 2008.

[17] R. Tandra and A. Sahai, "SNR walls for signal detection," *IEEE Selected Topics in Signal Processing*, vol. 2, pp. 4–17, Feb 2008.

[18] W. Krenik and A. Batra, "Cognitive radio techniques for wide area networks," *Design Automation Conference*, Jun 2005.

[19] Y. Zhao, L. Morales, J. Gaeddert, K. Bae, J. Um, and J. H. Reed, "Applying radio environment maps to cognitive wireless regional area networks," *Proc. IEEE DySpan*, pp. 115–118, Apr 2007.

[20] D. Gurney, G. Buchwald, L. Ecklund, S. Kuffner, and J. Grosspietsch, "Geo-location database techniques for incumbent protection in the tv white space," *Proc. IEEE DySpan*, 2008.

[21] A. B. H. Alaya-Feki, B. Sayrac, S. B. Jemaa, and E. Moulines, "Interference cartography for hierarchical dynamic spectrum access," *Proc. IEEE DySpan*, pp. 1–5, Oct 2008.

[22] B. Wild and K. Ramchandran, "Detecting primary receivers for cognitive radio applications," *Proc. IEEE DySpan*, pp. 124–130, 2005.

[23] M. F. Hanif, M. S., P. J. Smith, and P. A. Dmochowski, "Interference and deployment issues for cognitive radio systems in shadowing environments," *Proc. IEEE Int. Conf. on Comm. (ICC)*, 2009.

[24] M. F. Hanif, P. J. Smith, and M. Shafi, "Performance of cognitive radio systems with imperfect radio environment map information," *Proc. Australian communication theory workshop, Sydney*, pp. 61–66, Feb 2009.

[25] D. Molkdar, "Review on radio propagation into and within buildings," *Microwaves, Antennas and Propagation, IEE Proceedings*, vol. 138, pp. 61– 73, Feb 1991.

[26] D. Stoyan, W. S. Kendall, and J. Mecke, *Stochastic Geometry and its Applications*, John Wiely & Sons, Ltd, 1995.

[27] F. Baccelli, B. Blaszczyszyn, and P. Muhlethaler, "An aloha protocol for multihop mobile wireless networks," *IEEE Trans. Infomation Theory*, vol. 52, pp. 421–436, Feb 2006.

[28] S. P. Weber, J. G. Andrews, and N. Jindal, "The effect of fading, channel inversion, and threshold scheduling on ad hoc networks," *IEEE Trans. Infomation Theory*, vol. 53, pp. 4127–4149, Nov 2007.

[29] H. Liu, H. Darabi, P. Banerjee, and J. Liu, "Survey of wireless indoor positioning techniques and systems," *IEEE Transactions on Systems, Man, and Cybernetics, Part C: Applications and Reviews*, vol. 37, pp. 1067 – 1080, Nov 2007.

[30] "Tv detection," Available at http://www.tvlicensing.biz/detection/.

[31] "Bluetooth specification," Available at http://www.bluetooth.com.

[32] P. Bahl, R. Chandra, T. Moscibroda, R. Murty, and M. Welsh, "White space networking with wi-fi like connectivity," *ACM SIGCOMM*, vol. 39, Oct 2009.

[33] Y. Kim and G. de Veciana, "Understanding the design space for cognitive networks," *Sixth Workshop on Spatial Stochastic Models for Wireless Networks (SpaSWiN)*, June 2010.

[34] S. R. Kulkarni and P. Viswanath, "A deterministic approach to throughput scaling in wireless networks," *IEEE Trans. Infomation Theory*, vol. 50, no. 6, pp. 1041–1049, Jun 2004.

[35] U. Kozat and L. Tassiulas, "Throughput capacity of random ad hoc networks with infrastructure support," in *MobiCom '03: Proceedings of the 9th annual international conference on Mobile computing and networking*, New York, NY, USA, 2003, pp. 55–65, ACM.

[36] A. Hasan and J. G. Andrews, "The guard zone in wireless ad hoc networks," *IEEE Trans. Wireless Comm.*, vol. 6, no. 3, pp. 897–906, March 2007.

[37] T. M. Cover and J. A. Thomas, *Elements of information theory*, WILEY, 2 edition, 2006.

[38] Y. Kim and G. de Veciana, "Capacity region of cognitive networks heterogeneous environment and context awareness," *Technical Report*, 2010
Available at http://users.ece.utexas.edu/~ykim2/Kim10TR.pdf.

[39] A. Jovičić and P. Viswanath, "Cognitive radio: An information- theoretic perspective," *IEEE Trans. Infomation Theory*, vol. 55, no. 9, pp. 3945–3958, Sep 2009.

[40] M. F. Hanif and P. J. Smith, "On the statistics of cognitive radio capacity in shadowing and fast fading environments," *IEEE Trans. Wireless Comm.*, vol. 9, no. 2, pp. 844–852, Feb 2010.

[41] S. M. Ross, *Stochstic Processes*, John Wiley & Sons, Inc, 1983.

[42] D. Stoyan, *Comparison methods for queues and other stochastic models*, John Wiley & Sons, 1983.

APPENDIX A
PROOF OF THEOREM 1

Proof: We define following for notational simplicity:

$$\begin{aligned}
\mathcal{K}_1 &\equiv K\left(X, r_d; Y, r_{sp}(d)\right), \\
\mathcal{K}_2 &\equiv K\left(X, r_d^i; Y, r_{sp}^i(d)\right), \\
A &\equiv \{Y \textit{ not} \text{ interfered by active E-STxs}\} \\
&= \left\{Y \notin B\left(\Pi'_{so}, r_{sp}\right), Y \notin B\left(\Pi'_{si}, r_{sp}^i\right)\right\}, \text{ and} \\
B &\equiv \{\|X - Y\| = d\}.
\end{aligned}$$

Suppose that a PRx Y is located a distance $d \le d_p$ from its nearest PTx X as shown in Fig.8a. Conditioning on this event means that there are no PTxs within $b(Y, d)$; this is exhibited as a shaded disc in Fig. 8a. The PRx Y can be interfered by potential E-oSTxs in $\mathcal{K}_1$ and E-iSTxs in $\mathcal{K}_2$. Note, however, that not all E-STxs in $\mathcal{K}_1$ and $\mathcal{K}_2$ are active since to be active they require a PTx free area around them. For example, in Fig.8a, an E-oSTx z requires the region $b(z, r_d)$ be PTx free. Similarly, an E-iSTx z requires the region $b\left(z, r_d^i\right)$ be PTx free. So, the conditional outage probability given the event B is given by $P_{out}^p(d) = P(Y \text{ fails to receive } |B) = 1 - P(A|B)$, where $P(A|B)$ is computed as follows:

$$\begin{aligned}
P(A|B) &\stackrel{a}{=} \mathbb{E}[P(A|B\Pi_p)|B] \\
&\stackrel{b}{=} \mathbb{E}\big[P\left(Y \notin B\left(\Pi'_{so}, r_{sp}\right)|B\Pi_p\right) \times \\
&\qquad P\left(Y \notin B\left(\Pi'_{si}, r_{sp}^i\right)|B\Pi_p\right)|B\big] \\
&\stackrel{c}{=} \mathbb{E}\Big[\exp\Big\{-\int_{\mathcal{K}_1} \lambda_{so}\mathbf{1}\{z \notin B(\Pi_p^{(2)}, r_d)\}dz\Big\} \times \\
&\qquad \exp\Big\{-\int_{\mathcal{K}_2} \lambda_{si}\mathbf{1}\{z \notin B(\Pi_p^{(2)}, r_d^i)\}dz\Big\}|B\Big] \\
&\stackrel{d}{=} \mathbb{E}\Big[\exp\{-\lambda_s(a_o L_1(d, \Pi_p^{(2)}) + a_i L_2(d, \Pi_p^{(2)}))\}\Big]
\end{aligned}$$

In $\stackrel{a}{=}$, we conditioned on Π_p, since event A depends on Π_p (note that Π'_{so} and Π'_{si} are processes depending on Π_p). In $\stackrel{b}{=}$, we used the fact that the events $\{Y \notin B(\Pi'_{so}, r_{sp})\} = \{\Pi'_{so} \cap b(Y, r_{sp}) = \emptyset\}$ and $\left\{Y \notin B\left(\Pi'_{si}, r_{sp}^i\right)\right\} = \left\{\Pi'_{si} \cap b(Y, r_{sp}^i) = \emptyset\right\}$ are conditionally independent given Π_p. In other words, for given primary transmitters' locations, the locations of active indoor nodes and outdoor nodes are independent. In $\stackrel{c}{=}$, the two outage probabilities are given as the void probabilities of random areas which should not be covered by PTx process $\Pi_p^{(2)}$ out of $\mathcal{K}_1$ and $\mathcal{K}_2$ respectively. For simplicity we define $\Pi_p^{(2)}$ as Π_p conditioned on B. In $\stackrel{d}{=}$, the expectation $\mathbb{E}$ is w.r.t. to a new conditioned random process $\Pi_p^{(2)}$, so we remove conditioning. If $d > d_p$, the PRx is out of PTx coverage area, so $P_{out}^p(d) = 0$. ■

APPENDIX B
PROOF OF THEOREM 6

Proof: Suppose that an E-oSTx Z_o detects the absence of PTxs in its detection range $b\left(Z_o, r_d^{\mathrm{E}}\right)$ as shown in Fig.9. Consider Z_o's intended receiver E-oSRx W_o which is a distance d_s from Z_o. Then, the conditional outage probability $P_{out}^{so\mathrm{E}}$ is given as

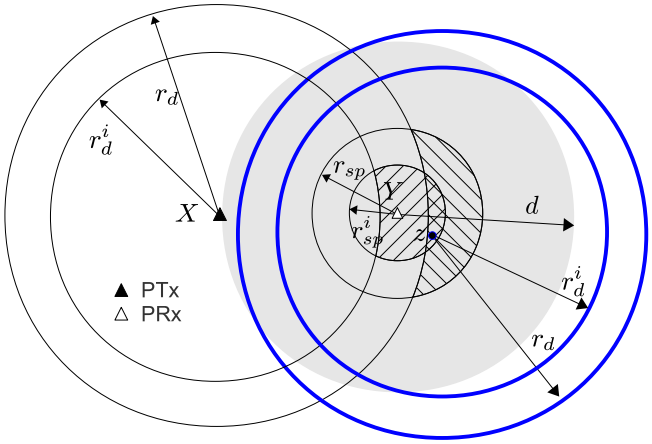

(a) By conditioning PRx Y at distance d to its nearest PTx X, we have no PTx in shaded region $b\left(Y,d\right)$. A PRx Y can be interfered by potential E-oSTxs in hatched region $\mathcal{K}_1 = b\left(Y,r_{sp}\right)\setminus b\left(X,r_d\right)$ or E-iSTxs in hatched region $\mathcal{K}_2 = b\left(Y,r_{sp}^i\right)\setminus b\left(X,r_d^i\right)$. The activity of potentially harmful E-iSTxs and E-oSTxs are affected by surrounding PTxs, e.g., E-oSTx z is active only when there is no PTxs in $b\left(z,r_d\right)$.

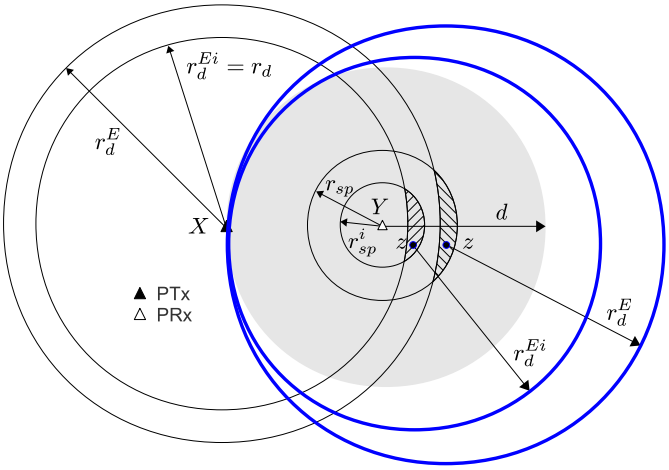

(b) By conditioning PRx Y at distance d to its nearest PTx X, we have no PTx in shaded region $b\left(Y,d\right)$. A PRx Y can be interfered by potential E-oSTxs in hatched region $\mathcal{K}_3 = b\left(Y,r_{sp}\right)\setminus b\left(X,r_d^E\right)$ or E-iSTxs in hatched region $\mathcal{K}_2 = b\left(Y,r_{sp}^i\right)\setminus b\left(X,r_d^{Ei}\right)$. The activity of potential E-iSTxs and E-oSTxs are affected by surrounding PTxs, e.g., E-oSTx z is active only when there is no PTxs in $b\left(z,r_d^E\right)$.

Fig. 8: PTx X and PRx Y were shown with E-STxs using signal energy detection method. Left figure corresponds to the case with detection radius considering only outdoor devices in Section IV-A and right figure corresponds to the case with conservative detection radius in Section IV-B.

Then, P_{out}^{soE} can be written as

$$\begin{aligned} P_{out}^{soE} &\overset{a}{=} 1 - P\left(W_o \text{ receives}|F\right) \\ &= 1 - P\left(D|EF\right)P\left(E|F\right) \end{aligned}$$

where in $\overset{a}{=}$, we omitted conditioning on $\{\|Z_o - W_o\| = d_s\}$ for notational simplicity. $P\left(E|F\right)$ and $P\left(D|EF\right)$ can be computed as follows:

$$\begin{aligned} P(E|F) &= P(W_o \notin B(\Pi_p, r_{ps})|Z_i \notin B(\Pi_p, r_d^{\mathrm{E}})) \\ &= \exp\{-\lambda_p|K(Z_o, r_d^{\mathrm{E}}, W_o, r_{ps})|\} = 1. \end{aligned} \tag{10}$$

Note that for a given parameter set or a scenario of interest, we have $\|K(Z_o, r_d^{\mathrm{E}}, W_o, r_{ps})| = 0$ since detection radius r_d^{E} is much larger than the interference radius r_{ps}, which results in $P\left(E|F\right) = 1$ in (10). Recall that $r_d^{\mathrm{E}} \geq r_{ps} + d_s$ guarantees the absence of hidden PTxs and therefore there is no negative impact from such PTxs. Thus we have that

$$\begin{aligned} &P\left(D|EF\right) \\ &\overset{a}{=} \mathbb{E}\left[P(W_o \notin B(\Pi_{so}^{\mathrm{E}}, r_{ss}^{oo}), W_o \notin B(\Pi_{si}^{\mathrm{E}}, r_{ss}^{io})|EF\Pi_p)|EF\right] \\ &\overset{b}{=} \mathbb{E}\big[P(W_o \notin B(\Pi_{so}^{\mathrm{E}}, r_{ss}^{oo})|EF, \Pi_p)\times \\ &\qquad\qquad P(W_o \notin B(\Pi_{si}^{\mathrm{E}}, r_{ss}^{io})|EF, \Pi_p)|EF\big] \\ &\overset{c}{=} \mathbb{E}\Big[\exp\Big\{-\int_{b(W_o, r_{ss}^{oo})} \lambda_{so}\mathbf{1}\left\{z \notin B\left(\Pi_p^{(3)}, r_d^{\mathrm{E}}\right)\right\}dz\Big\}\times \\ &\qquad \exp\Big\{-\int_{b(W_o, r_{ss}^{io})} \lambda_{si}\mathbf{1}\left\{z \notin B\left(\Pi_p^{(3)}, r_d^{\mathrm{E}i}\right)\right\}dz\Big\}|EF\Big] \\ &\overset{d}{=} \mathbb{E}\Big[\exp\{-\lambda_s(a_o Q(r_{ss}^{oo}, \Pi_p^{(3)}, r_d^{\mathrm{E}}) + a_i Q(r_{ss}^{io}, \Pi_p^{(3)}, r_d^{\mathrm{E}i}))\}\Big]. \end{aligned}$$

In the above equality $\overset{a}{=}$, we used conditional expectation $\mathbb{E}$ given the event EF. In $\overset{b}{=}$, we used the fact that the two events are conditionally independent given Π_p and in $\overset{c}{=}$, the probability that W_o is not covered by the Boolean process $B\left(\Pi_{so}^{\mathrm{E}}, r_{ss}^{oo}\right)$ is given as the void probability of the random subset of $b(W_o, r_{ss}^{oo})$. The second probability is also computed in the same fashion. Furthermore we used the fact that Π_p conditioned on EF is the same as $\Pi_p^{(3)}$. In $\overset{d}{=}$, $\mathbb{E}$ is taken w.r.t. the new random process $\Pi_p^{(3)}$. This completes the proof. ■

$P\left(W_o \text{ fails to receive}|Z_o \text{ transmits}, \|Z_o - W_o\| = d_s\right)$.
For notational simplicity we define following three events valid only in this proof:

$$\begin{aligned} D &\equiv \{W_o \textit{ not} \text{ interfered by active STxs}\} \\ &= \left\{W_o \notin B\left(\Pi_{so}^{\mathrm{E}}, r_{ss}^{oo}\right), W_o \notin B\left(\Pi_{si}^{\mathrm{E}}, r_{ss}^{io}\right)\right\}, \\ E &\equiv \{W_o \textit{ not} \text{ interfered by PTx}\} \\ &= \left\{W_o \notin B\left(\Pi_p, r_{ps}\right)\right\}, \text{and} \\ F &\equiv \left\{Z_o \textit{ not} \text{ detects PTx in } b\left(Z_o, r_d^{\mathrm{E}}\right)\right\} \\ &= \left\{Z_o \notin B\left(\Pi_p, r_d^{\mathrm{E}}\right)\right\}. \end{aligned}$$

APPENDIX C
PROOF OF THEOREM 10

Proof: Suppose that a G-oSTx Z_o detects the absence of PTxs in its detection radius $b\left(Z_o, r_d\right)$ as shown in Fig.10. Consider Z_o's intended receiver G-oSRx W_o which is at distance d_s from Z_o. Then, the conditional outage probability P_{out}^{soG} is given by $P\left(W_o \text{ fails to receive}|Z_o \text{ transmits}, \|Z_o - W_o\| = d_s\right)$. For notational simplicity we define the following three events

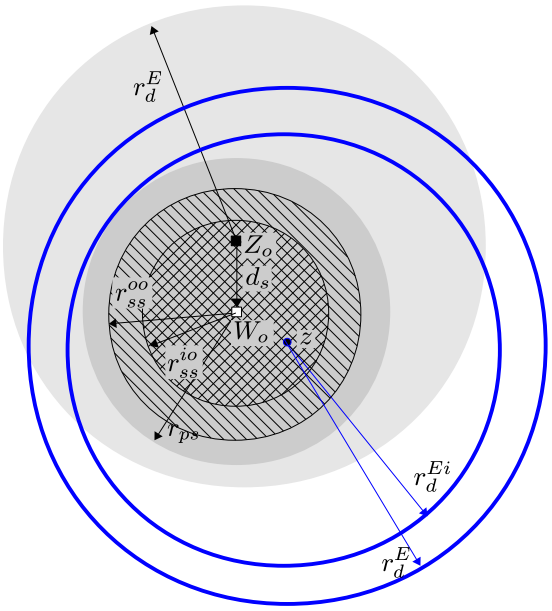

Fig. 9: Conditioned that there are no PTxs in $b\left(Z_o, r_d^E\right)(\supset b\left(W_o, r_{ps}\right))$, an E-oSRx W_o can be interfered by potential E-oSTxs in $b\left(W_o, r_{ss}^{oo}\right)$ or potential E-iSTxs in $b\left(W_o, r_{ss}^{io}\right)$. Their activities are determined by surrounding PTxs in $b\left(z, r_d^E\right)$ for E-oSTxs and $b\left(z, r_d^{Ei}\right)$ for E-iSTxs.

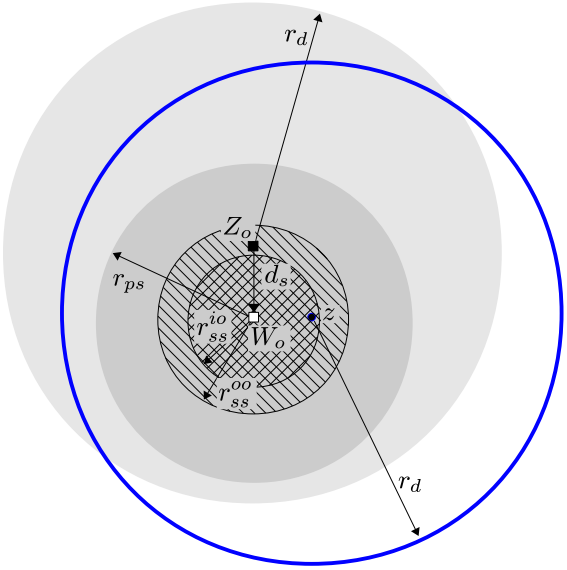

Fig. 10: Conditioned that there are no PTxs in $b\left(Z_o, r_d\right)(\supset b\left(W_o, r_{ps}\right))$, a G-oSRx W_o can be interfered by potential G-oSTx in $b\left(W_o, r_{ss}^{oo}\right)$ or G-iSTxs in $b\left(W_o, r_{ss}^{io}\right)$. The activity of potential G-oSTxs(G-iSTxs) are affected by surrounding PTxs, e.g., a G-oSTx(G-iSTx) at z can be preempted by PTxs inside $b(z, r_d)$.

valid only in this proof:

$$\begin{aligned}
D &\equiv \{W_o \text{ is } \textit{not} \text{ interfered by any G-STx}\} \\
&= \left\{W_o \notin B\left(\Pi_{so}^{\mathrm{G}}, r_{ss}^{oo}\right), W_o \notin B\left(\Pi_{si}^{\mathrm{G}}, r_{ss}^{io}\right)\right\}, \\
E &\equiv \{W_o \text{ is } \textit{not} \text{ interfered by any PTx}\} \\
&= \left\{W_o \notin B\left(\Pi_p, r_{ps}\right)\right\}, \text{ and} \\
F &\equiv \left\{Z_o \text{ does } \textit{not} \text{ detect any PTx in } b\left(Z_o, r_d\right)\right\} \\
&= \left\{Z_o \notin B\left(\Pi_p, r_d\right)\right\}.
\end{aligned}$$

The probability of outage $P_{out}^{so\mathrm{G}}$ can be written as $P_{out}^{so\mathrm{G}} \stackrel{a}{=} 1 - P\left(W_o \text{ receives}|F\right) = 1 - P\left(D|EF\right)P\left(E|F\right)$, where the equality $\stackrel{a}{=}$ follows by omitting conditioning on $\{\|Z_o - W_o\| = d_s\}$ for notational simplicity. $P\left(E|F\right)$ and $P\left(D|EF\right)$ are computed as follows:

$$\begin{aligned}
P\left(E|F\right) &= P\left(W_o \notin B\left(\Pi_p, r_{ps}\right)|Z_o \notin B\left(\Pi_p, r_d\right)\right) \\
&= \exp\left\{-\lambda_p\left|K\left(Z_o, r_d, W_o, r_{ps}\right)\right|\right\} = 1.
\end{aligned}$$

$$\begin{aligned}
&P\left(D|EF\right) \\
&\stackrel{a}{=} \mathbb{E}\left[P(W_o \notin B(\Pi_{so}^{\mathrm{G}}, r_{ss}^{oo}), W_o \notin B(\Pi_{si}^{\mathrm{G}}, r_{ss}^{io})|EF\Pi_p)|EF\right] \\
&\stackrel{b}{=} \mathbb{E}\Big[P\left(W_o \notin B\left(\Pi_{so}^{\mathrm{G}}, r_{ss}^{oo}\right)|EF\Pi_p\right) \times \\
&\qquad P\left(W_o \notin B\left(\Pi_{si}^{\mathrm{G}}, r_{ss}^{io}\right)|EF\Pi_p\right)|EF\Big] \\
&\stackrel{c}{=} \mathbb{E}\Big[\exp\Big\{-\int_{b(W_o, r_{ss}^{oo})} \lambda_{so}\mathbf{1}\left\{z \notin B\left(\Pi_p^{(4)}, r_d\right)\right\}dz\Big\} \times \\
&\qquad \exp\Big\{-\int_{b(W_o, r_{ss}^{io})} \lambda_{si}\mathbf{1}\left\{z \notin B\left(\Pi_p^{(4)}, r_d\right)\right\}dz\Big\}|EF\Big] \\
&= \mathbb{E}\left[\exp\{-\lambda_s(a_o Q(r_{ss}^{oo}, \Pi_p^{(4)}, r_d) + a_i Q(r_{ss}^{io}, \Pi_p^{(4)}, r_d))\}\right]
\end{aligned}$$

In the above equality $\stackrel{a}{=}$, $\mathbb{E}$ is a conditional expectation conditioned on E and F. In $\stackrel{b}{=}$, two events are conditionally independent given Π_p and in $\stackrel{c}{=}$, Π_p conditioned on EF is the same as $\Pi_p^{(4)}$. ■

APPENDIX D
PROOF OF THEOREM 14

Proof: We condition on that an L-oSRx W_o is located a distance $d(\geq s_o)$ away from its nearest PTx as shown in Fig.11. This ensures that there is no PTx in a shaded disc $b\left(W_o, s_o\right)$. Note that our scenario (or parameter selection) guarantees $b\left(W_o, s_o\right) \supset b\left(Z_o, r_d^{\mathrm{L}}\right)$. An associated L-oSTx Z_o is located a distance d_s from the L-oSRx W_o. Then, the conditional outage probability $P_{out}^{so\mathrm{L}}(d)$ is given by $P(W_o \text{ fails to receive}|Z_o \text{ transmits}, \|Z_o - W_o\| = d_s, d \geq s_o)$. For notational simplicity we define the following events valid only in this proof:

$$\begin{aligned}
D &\equiv \{W_o \text{ is } \textit{not} \text{ interfered by any L-STx}\} \\
&= \left\{W_o \notin B\left(\Pi_{so}^{\mathrm{L}}, r_{ss}^{oo}\right), W_o \notin B\left(\Pi_{si}^{\mathrm{L}}, r_{ss}^{io}\right)\right\}, \\
E &\equiv \{W_o \text{ is } \textit{not} \text{ interfered by any PTx}\} \\
&= \left\{W_o \notin B\left(\Pi_p, r_{ps}\right)\right\}, \\
F &\equiv \left\{Z_o \text{ does } \textit{not} \text{ detect any PTx in } b\left(Z_o, r_d^{\mathrm{L}}\right)\right\} \\
&= \left\{Z_o \notin B\left(\Pi_p, r_d^{\mathrm{L}}\right)\right\}, \text{and} \\
G &\equiv \{d \geq s_o\} = \left\{W_o \notin B\left(\Pi_p, s_o\right)\right\}.
\end{aligned}$$

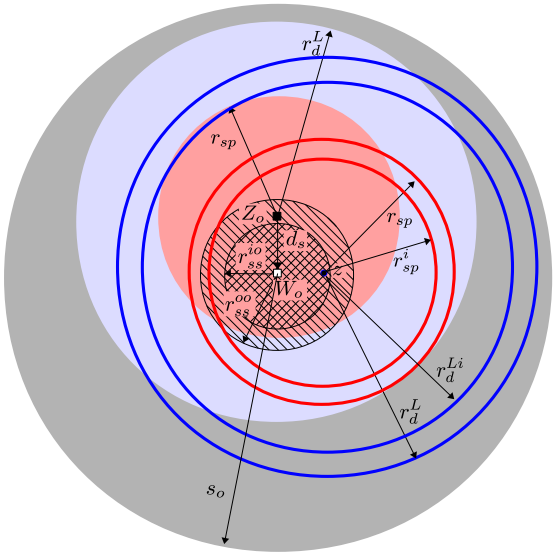

Fig. 11: Conditioned that there are no PTxs in $b\left(W_o, s_o\right)\left(\supset b\left(Z_o, r_d^L\right)\right)$, a L-oSRx W_o can be interfered by potential L-oSTx in $b\left(W_o, r_{ss}^{oo}\right)$ or L-iSTxs in $b\left(W_o, r_{ss}^{io}\right)$. Their activities are determined by surrounding PTxs, e.g., PTxs in $b\left(z, r_d^L\right)$ for a L-oSTx at z and PTxs in $b\left(z, r_d^{Li}\right)$ for a L-iSTx at z. However, no PRxs outside of coverage and $r_{ss}^{oo} + r_d^L < s_o$ in our scenario guarantee that all harmful L-STxs are active.

Then, the outage probability is given by

$$\begin{aligned} P_{out}^{so\mathrm{L}}(d) &= 1 - P\left(W_o \text{ receives} | FG\right) \\ &= 1 - P\left(DE|FG\right) \\ &= 1 - P\left(D|EFG\right) P\left(E|FG\right), \end{aligned}$$

where $P(E|FG)$ and $P(D|EFG)$ can be computed as

$$\begin{aligned} &P(E|FG) \\ &\quad = \exp\{-\lambda_p \pi |b(W_o, r_{ps}) \backslash \{b(Z_o, r_d^{\mathrm{L}}) \cup b(W_o, s_o)\}|\} = 1, \end{aligned}$$

$$\begin{aligned} &P(D|EFG) \\ &= \mathbb{E}[P(W_o \notin B(\Pi_{so}^{\mathrm{L}}, r_{ss}^{oo}), \\ &\qquad\qquad W_o \notin B(\Pi_{si}^{\mathrm{L}}, r_{ss}^{io}) | EFG\Pi_p) | EFG] \\ &\overset{a}{=} \mathbb{E}[P(W_o \notin B(\Pi_{so}^{\mathrm{L}}, r_{ss}^{oo}) | EFG\Pi_p) \\ &\qquad\qquad \times P(W_o \notin B(\Pi_{si}^{\mathrm{L}}, r_{ss}^{io}) | EFG\Pi_p) | EFG] \\ &\overset{b}{=} \mathbb{E}\Big[\exp\Big\{-\int_{\mathcal{K}_4} \lambda_{so} \mathbf{1}\{T_o(z, \Pi_r)\} \mathbf{1}\{z \notin B(\Pi_p^{(5)}, r_d^{\mathrm{L}})\} dz\Big\} \times \\ &\exp\Big\{-\int_{\mathcal{K}_4} \lambda_{si} \mathbf{1}\{T_i(z, \Pi_r)\} \mathbf{1}\{z \notin B(\Pi_p^{(5)}, r_d^{\mathrm{L}i})\} dz\Big\} | EFG\Big] \\ &\overset{c}{=} \mathbb{E}\Big[\exp\{-\lambda_{so} Q(r_{ss}^{oo}, \Pi_p^{(5)}, r_d^{\mathrm{L}})\} \\ &\qquad\qquad \times \exp\{-\lambda_{si} Q(r_{ss}^{io}, \Pi_p^{(5)}, r_d^{\mathrm{L}i})\} | EFG\Big] \\ &\overset{d}{=} \mathbb{E}\big[\exp\{-\lambda_s (a_o Q(r_{ss}^{oo}, \Pi_p^{(5)}, r_d^{\mathrm{L}}) + a_i Q(r_{ss}^{io}, \Pi_p^{(5)}, r_d^{\mathrm{L}i}))\}\big]. \end{aligned}$$

In $\overset{a}{=}$, we use the fact that two events are conditionally independent. In $\overset{b}{=}$, we have $\mathcal{K}_4 = b(W_o, r_{ss}^{oo})$ and introduce Π_p conditioned on EFG which is denoted as $\Pi_p^{(5)}$. In $\overset{c}{=}$, we use the fact that $\mathbf{1}\left\{T_o\left(z, \Pi_r\right)\right\} = \mathbf{1}\left\{T_i\left(z, \Pi_r\right)\right\} = 1$ since W_o is in the outside of PTx's converge. In $\overset{d}{=}$, $\mathbb{E}$ is w.r.t. a new random process $\Pi_p^{(5)}$. This completes the proof. ■

Yuchul Kim Yuchul Kim received his B.S. degree from Korea University in 2000 and M.S. degree from Korea Advanced Institute of Science and Technology in 2003, all in Electrical Engineering. He is currently working toward his Ph.D. at The University of Texas at Austin. He had worked in Global Standardization and Research Lab in the Telecommunication and Network division of Samsung Electronics from 2003 to 2006. His research interests include the design, modeling and performance evaluation of wireless networks.

Gustavo de Veciana Gustavo de Veciana (S'88-M'94-SM'01-F'09) received his B.S., M.S, and Ph.D. in electrical engineering from the University of California at Berkeley in 1987, 1990, and 1993 respectively. He is currently a Professor at the Department of Electrical and Computer Engineering and recipient of the Temple Foundation Centennial Fellowship. He served as the Director and Associate Director of the Wireless Networking and Communications Group (WNCG) at the University of Texas at Austin, from 2003-2007. His research focuses on the design, analysis and control of telecommunication networks. Current interests include: measurement, modeling and performance evaluation; wireless and sensor networks; architectures and algorithms to design reliable computing and network systems. Dr. de Veciana has been an editor for the IEEE/ACM Transactions on Networking. He was the recipient of a National Science Foundation CAREER Award 1996, co-recipient of the IEEE William McCalla Best ICCAD Paper Award for 2000, and co-recipient of the Best Paper in ACM Transactions on Design Automation of Electronic Systems, Jan 2002-2004. In 2009 he was designated IEEE Fellow for his contributions to the analysis and design of communication networks.